

Transition Edge Sensors

Piet de Korte

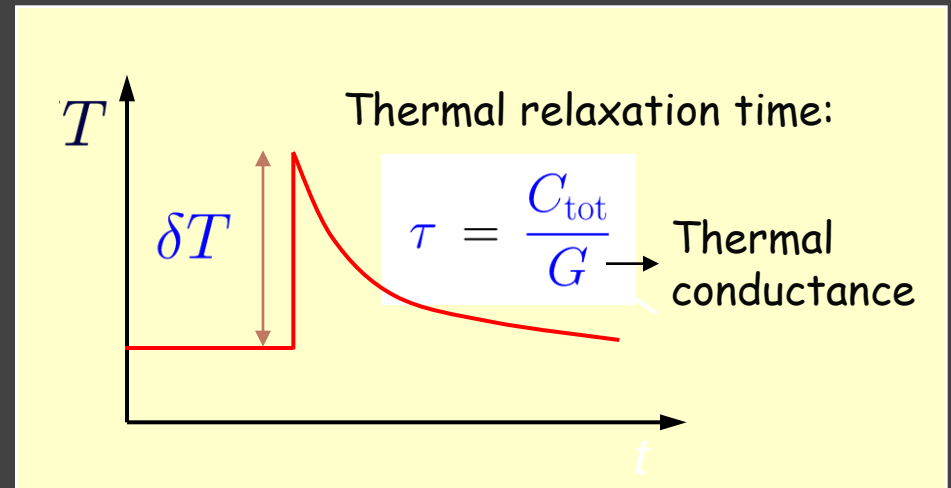
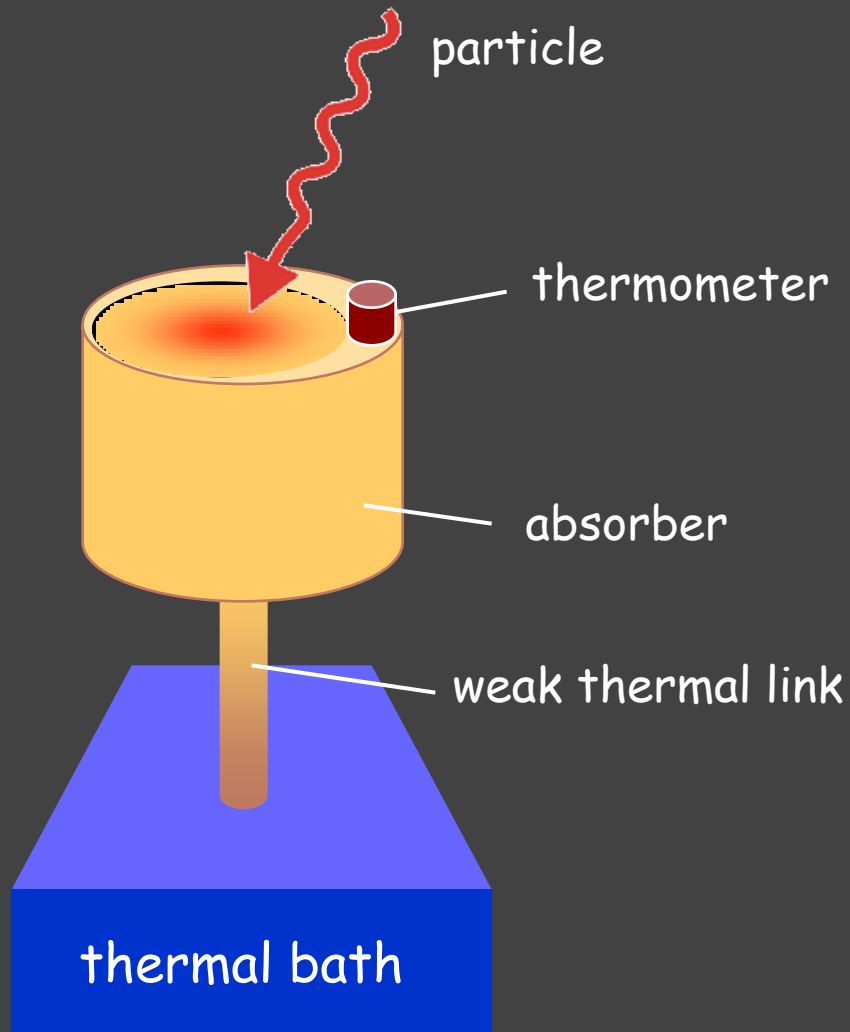
Literature/Acknowledgement

- Acknowledgement to Christian Enns and Dan McCammon for making available lecture material on TES-micro-calorimeters
- Acknowledgement to Marcel Bruijn and Bob Dirks for making sheets on the production process and on device characterization available
- For literature please read:
 - Transition-Edge Sensor by Kent Irwin and Gene Hilton in *Cryogenic Particle Detectors, Topics in Appl. Physics, Vol 99* Editor: Christian Enns, Springer Verlag (2005)
 - Proceedings of Low Temperature Detector (LTD) conferences and references in there

Content TES physics

- 1) Schematic of Calorimeter Principle
- 2) Electro-thermal feedback
- 3) Basic Pixel Design
 - 1) Heat Capacity
 - 2) Heat Conductance
 - 3) TES-bolometer
- 4) Differential equations
 - 1) Linearization
 - 2) Matrix notation in frequency domain
 - 3) Responsivity
 - 4) Noise
 - 5) Complex impedance
- 5) Energy resolution
 - 1) Time domain
 - 2) Frequency domain
- 6) Pixel characterization (example)

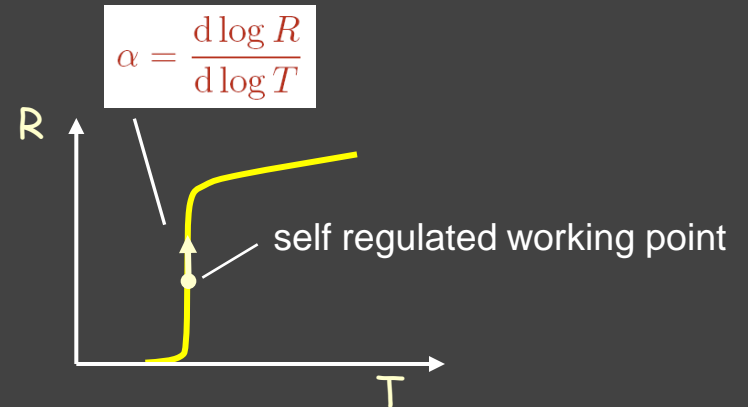
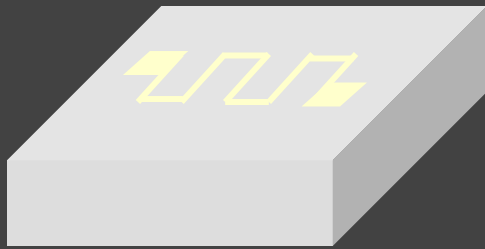
Calorimeter Principle



$$\delta T = \frac{E}{C_{\text{tot}}}$$

C_{tot} : phonons
electrons
spins
tunneling states
quasi particles

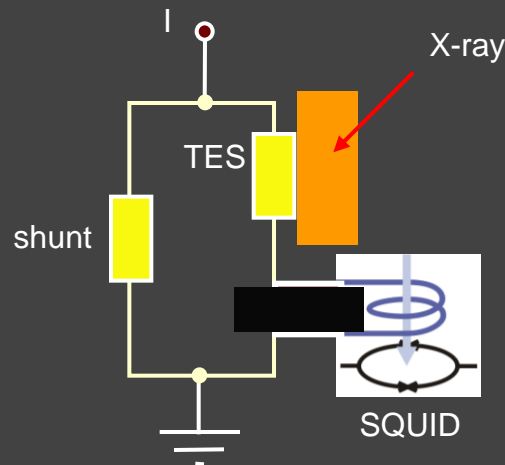
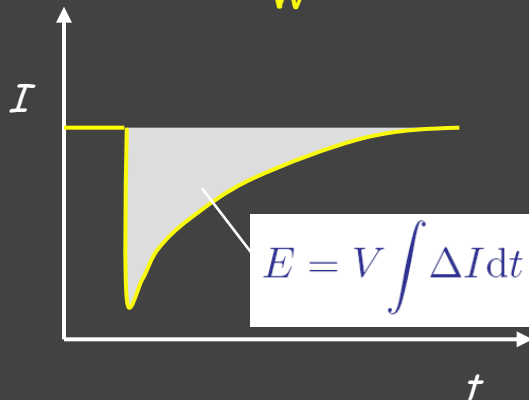
Superconducting Transition Edge Sensors (TES)



Materials Mo/Cu
Mo/Au
Ir/Au
Ti/Au
W

Electro-thermal feedback

K. D. Irwin, Appl. Phys. Lett. 66, 1945 (1995)



heat input:

- R_{TES} goes up
- joule heating decreases

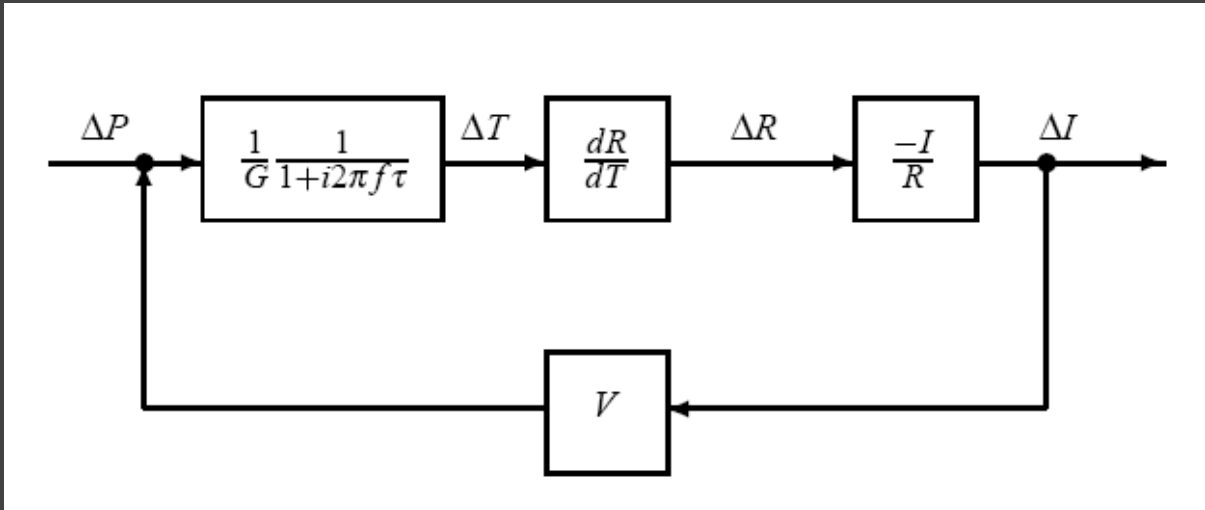
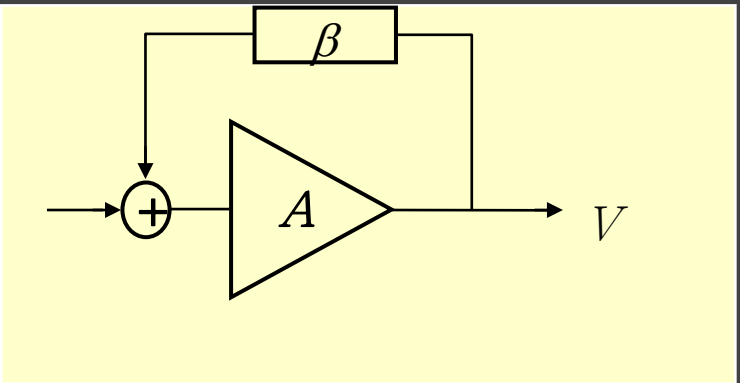
fast response time

$$\tau_{\text{eff}} = \frac{\tau}{1 + \alpha/n}$$

$$G \propto T^{n-1}$$

Electro-thermal Feedback

$$S = \frac{V_{out}}{V_{in}} = \frac{1}{\beta} \frac{A\beta}{1 + A\beta}$$



$$L = \frac{1}{G} \frac{R\alpha}{T} \frac{-I}{R} \frac{V}{1 + \omega\tau} = -\frac{\alpha P}{GT} \frac{1}{1 + \omega\tau} = \frac{L_0}{1 + \omega\tau}$$

$$S_I \equiv \frac{dI}{dP} = \frac{1}{V} \frac{L}{1 + L} = \frac{1}{V} \frac{L_0}{1 + L_0} \frac{1}{1 + \omega\tau / (1 + L_0)}$$

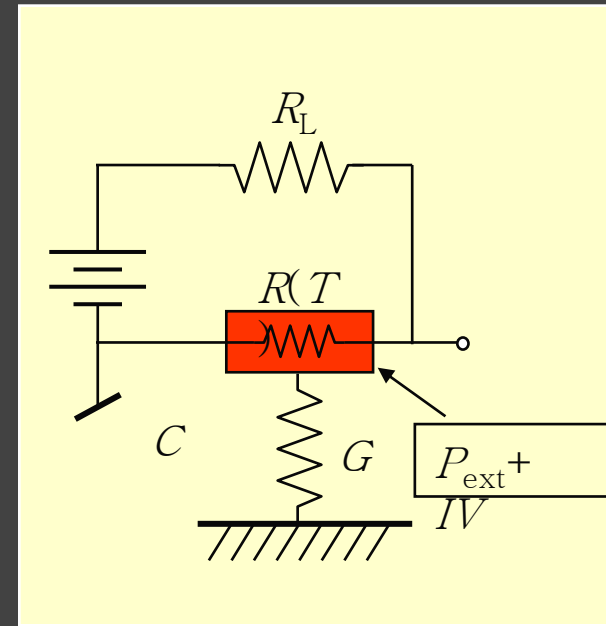
Open loop gain

$$L_0 = \alpha P / GT$$

$$P = K(T^n - T_0^n)$$

$$G = nKT^{n-1}$$

$$L_0 = \frac{\alpha}{n} \left[1 - \left(\frac{T}{T_0} \right)^n \right] \approx \alpha / n$$



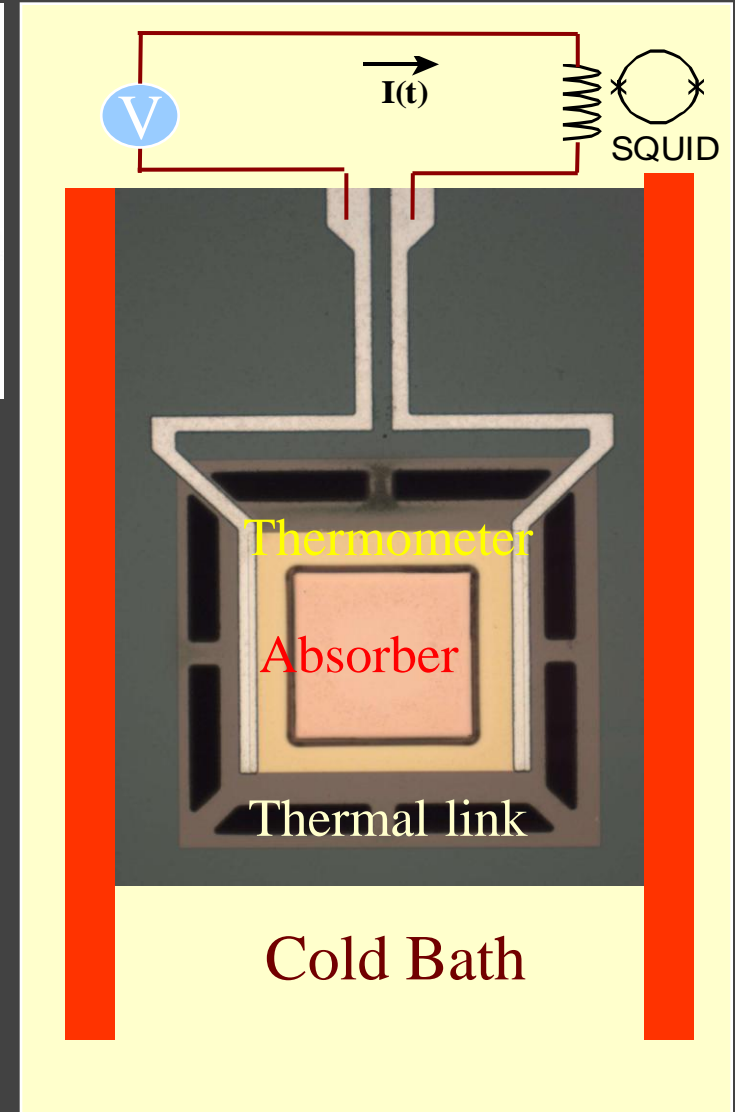
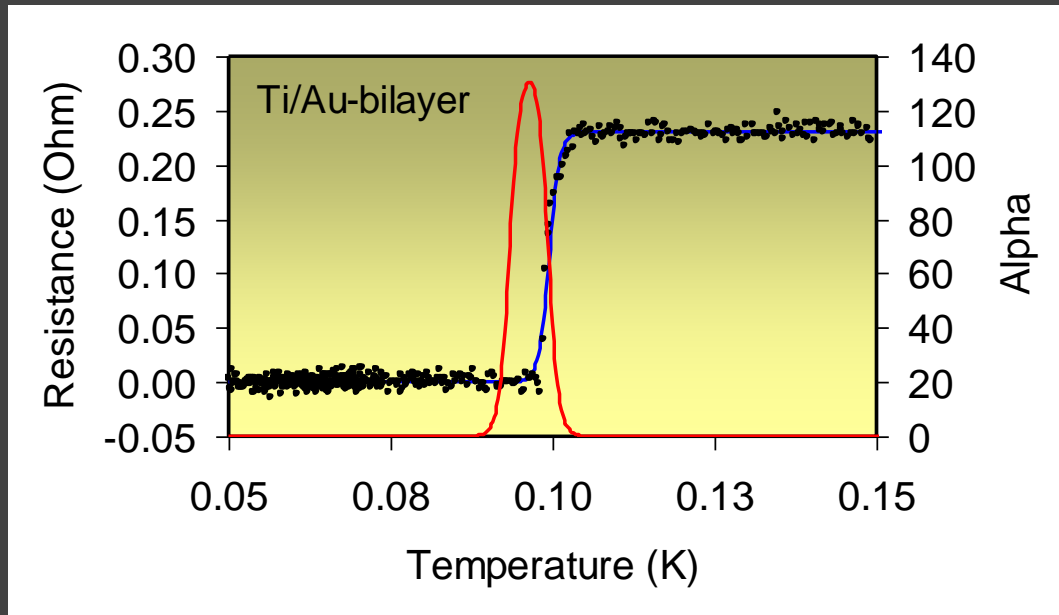
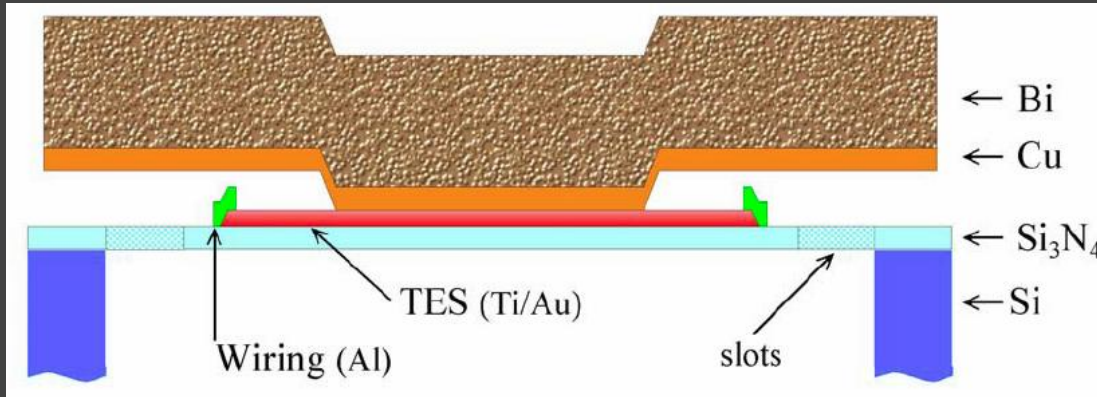
$$F_L = \frac{R - R_L}{R + R_L}$$

Influence load resistor

$$L = L \cdot F_L$$

TES-based Micro-Calorimeter

BASIC PIXEL DESIGN



Typical Design parameters

- Heat Capacity
 - Electronic heat capacity $C = \gamma.T.V$ (γ the Sommerfeld parameter)
 - Phonon heat capacity $C = A.T^3.V$
 - For $T < 1$ K the C of normal metals is dominated by the electronic heat capacity (not for Bi)

Typical heat capacity of one pixel at $T = 100$ mK:

- TES $150 \times 150 \mu\text{m}$ of 25nm Ti ($\gamma = 315$) and 50 nm Au ($\gamma = 71$). An area of $100 \times 100 \mu\text{m}^2$ under stem is normal (N), the S-rim is biased at $R/R_n = 0.2$.
C superconductor phase = 2.43x that of normal phase

$$C_{\text{TES}} = 7 \cdot 10^{-14} \text{ J/K}$$

- Cu-conductor $250 \times 250 \mu\text{m}$ of $0.3 \mu\text{m}$ ($\gamma = 97$)

$$C_{\text{Cu}} = 1.8 \cdot 10^{-13} \text{ J/K}$$

- Bi-absorber $250 \times 250 \mu\text{m}$ of $3 \mu\text{m}$ ($\gamma = 3.9$??)

$$C_{\text{BI}} = 7.3 \cdot 10^{-14} \text{ J/K}$$

- SiN-membrane ($220 \times 180 \times 1 \mu\text{m}$)

$$C_{\text{SiN}} \approx 1 \cdot 10^{-13} \text{ J/K}$$

Total heat capacity/pixel

$$C_{\text{total}} = 0.42 \text{ pJ/K}$$

$$E_{\text{MAX}} = C.\delta T \approx CT/a \quad \text{For } a \approx T/\delta T \approx 100 \text{ we get } E_{\text{MAX}} \approx 2.6 \text{ keV}$$

Typical Design Parameters for heat transport

- Design of Heat Conductance value
 - Given typical electro-thermal feedback loop gains of 20x (eff. $\alpha = 100$)
 - Design a pixel with an effective time constant of 100 μ s
 - $\rightarrow C/G = 2$ ms or $\rightarrow G \approx 2.5 \cdot 10^{-10}$ W/K
- Heat transport
 - Generation of heat in electrical system of TES/absorber
 - Heat transport to bath by phonon's in membrane:
 - 1) e-ph coupling in TES/absorber $G_{e-ph} = n \cdot \Sigma \cdot VT^{n-1}$ with $n = 5$ and $\Sigma = 2 \cdot 10^9$ W/K⁵m³. So $\rightarrow G_{e-ph} \approx 2 \cdot 10^{-7}$ W/K
 - 2) Kapitza coupling to membrane $G_{kapitza} = n \cdot \alpha_K \cdot A \cdot T^{n-1}$ with $n = 4$. Typically $\alpha_K = 125$ W/K⁴m². So $G_{kapitza} = 1.12 \cdot 10^{-8}$ W/K
 - 3) Radiative phonon transport (Hoevers et al. Appl.Phys.Lett 86, 251903 (2005)) $G_{memb} = \xi \cdot \sigma_B \cdot n \cdot A_{ph} \cdot T^{n-1}$ W/K³m² with $n = 4$. Typically $\xi = 0.78$. The Stefan-Boltzmann constant for phonon transport equals $\sigma_B = 157$ W/K⁴m². So for $A_{ph} = 4 \times 150 \times 1 \mu\text{m}^2 \rightarrow G_{memb} = 2.9 \cdot 10^{-10}$ W/K
Reduction of this value is possible by structuring the SiN-membrane.
Typical $P \approx TG/n = 6$ pW

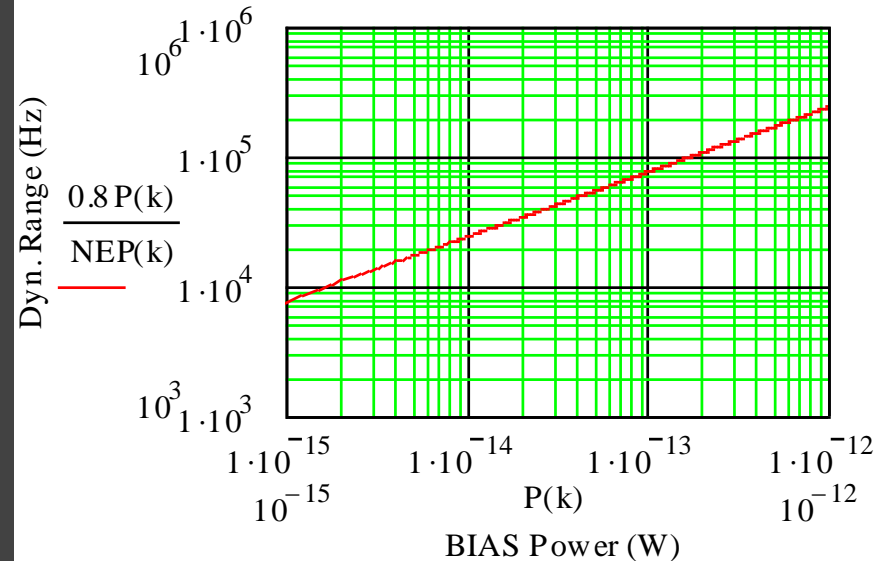
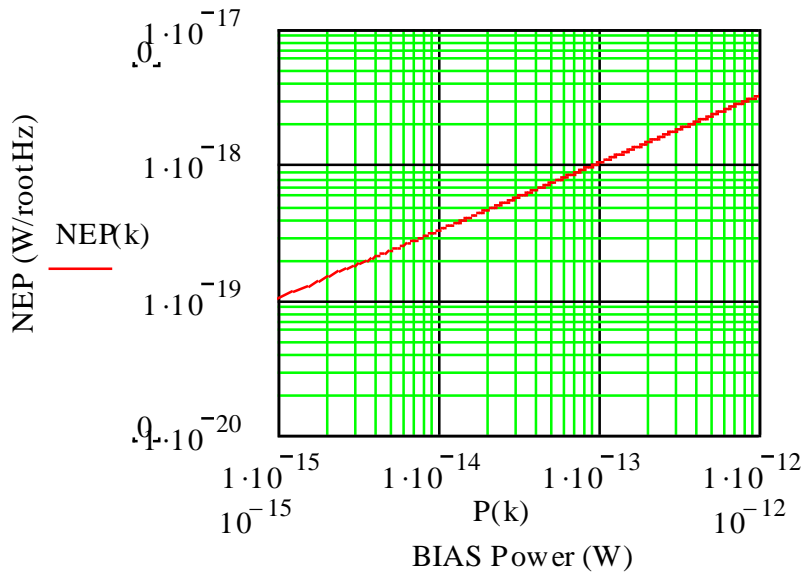
TES-Bolometer characteristics

- NEP and Dynamic Range

$$P = K(T^n - T_{\text{bath}}^n)$$

$$NEP = \sqrt{4\gamma k T^2 G} \cong \sqrt{4\gamma n k T P}$$

$$\frac{\Delta I}{i_n} = \frac{(1-r).P}{NEP} = (1-r) \sqrt{\frac{P}{4\gamma n k T}}$$



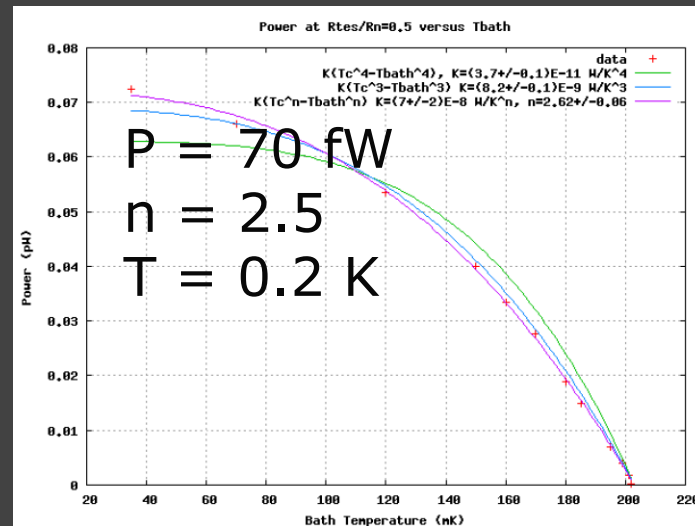
- Time constant

$$\tau_{\text{eff}} = \frac{C}{G} \frac{1}{1 + L_0} \cong \frac{CT}{\alpha P}$$

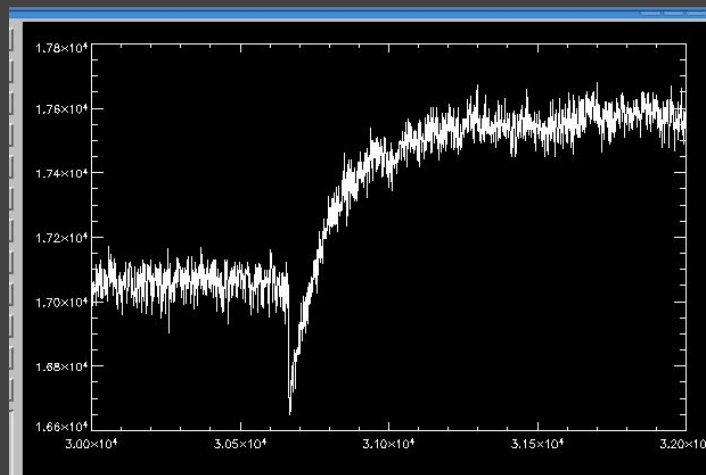
$$C/G \approx 4 \text{ ms}$$

$$NEP = 10^{-18} \text{ W}/\sqrt{\text{Hz}}$$

Low NEP TES-bolometer for SAFARI (SPICA)



$$NEP = \sqrt{4kT^2 P} \approx \sqrt{4kTP}$$



$T_C = 200 \text{ mK}$
 $100 \times 100 \text{ } \mu\text{m TES}$
 $4 \text{ legs of } 5 \text{ } \mu\text{m and}$
 1.8 mm

Measured
 $P = 70 \text{ fW}$
 $NEP = 10^{-18} \text{ W}/\sqrt{\text{Hz}}$
 $T_{\text{eff}} = 0.2 \text{ ms}$

Next steps:

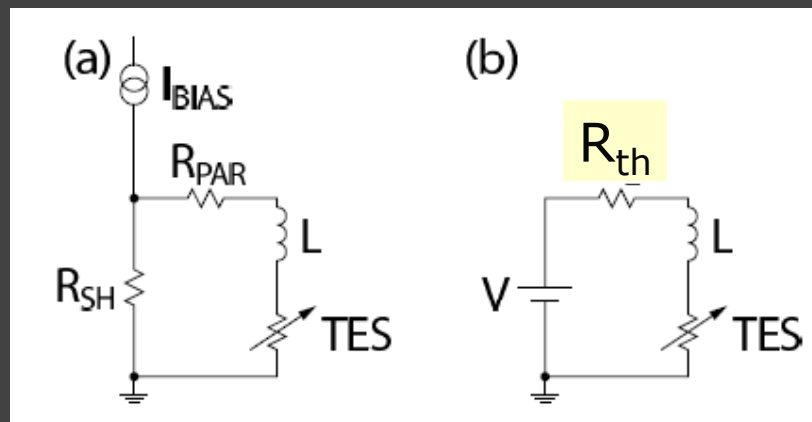
$T \rightarrow 100 \text{ mK}$
 $\text{Leg width} \rightarrow 2 \text{ } \mu\text{m}$

Differential Equations

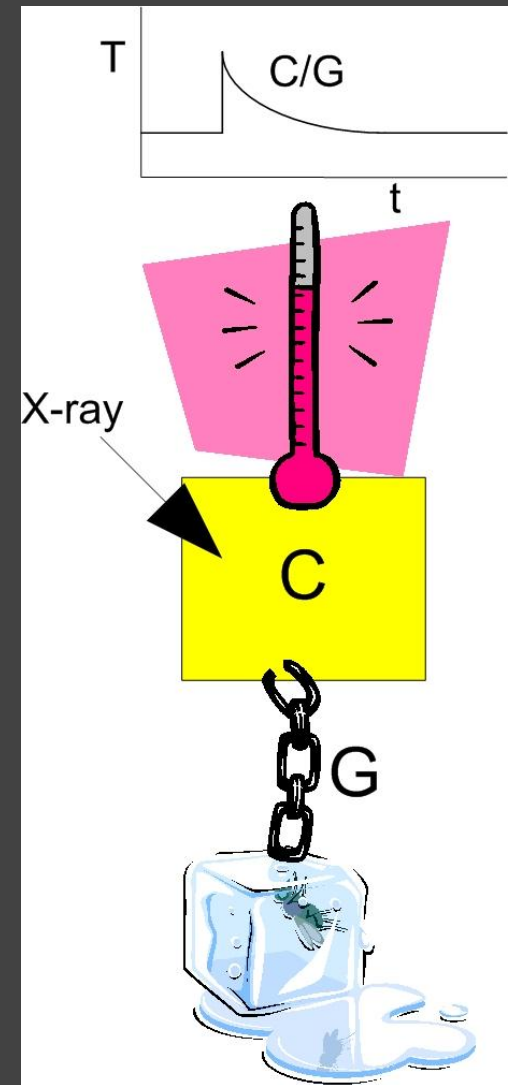
- Thermal differential equation

$$C \frac{dT}{dt} + P_{bath} + I_0 \cdot V_{Johnson} = P_{Joule} + P$$

- Electrical differential equation



$$L \frac{dI}{dT} + I \cdot R_{th} + I \cdot R(T, I) = V + V_{Johnson} + V_{Noise}$$



Linearizations (small signal approximation)

$$P_{bath} = K(T^n - T_{bath}^n)$$

$$G \equiv \frac{dP_{bath}}{dT} = nKT^{n-1}$$

$$P_{bath} \approx P_{bath0} + G \cdot \Delta T$$

n = 5 electron-phonon transport

n = 4 Kapitza boundary

n = 3 Phonon transport

$$R(T, I) \approx R_0 + \alpha_I \cdot \frac{R_0}{I_0} \cdot \Delta I + \alpha_T \cdot \frac{R_0}{T_0} \Delta T$$

Resistance does also depend on I through action of B-field

$$P_{Joule} = I^2 \cdot R = P_{J0} + 2 \cdot I_0 \cdot R_0 \cdot \Delta I + \alpha_I \cdot \frac{P_{J0}}{I_0} \cdot \Delta I + \alpha_T \cdot \frac{P_{J0}}{T_0} \cdot \Delta T$$

Matrix solution

$$\begin{bmatrix} \Delta I \\ \Delta T \end{bmatrix} \cdot \begin{bmatrix} i\omega L + R_{th} + R_0(1 + \alpha_I) & \frac{R_0 I_0}{T_0} \alpha_T \\ -R_0 I_0(2 + \alpha_I) & i\omega C + G - \frac{P_{J0} \alpha_T}{T_0} \end{bmatrix}^{-1} = \begin{bmatrix} V_{Johnson} + V_{noise} \\ -I_0 \cdot V_{Johnson} + P \end{bmatrix}$$

Responsivity

$$S_I \equiv \Delta I / P = M_{0,1}^{-1}$$

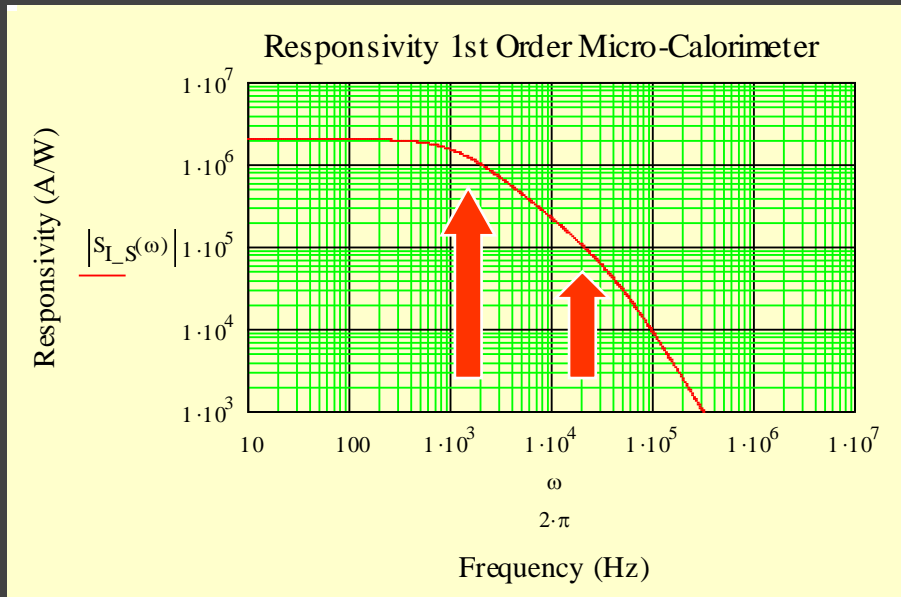
$$S_I = -\frac{1}{I_0 R_0} \left(\left(1 + \frac{1 + \alpha_I}{L_0} \right) (1 + i\omega \tau_{fall}) + \frac{R_{th} + i\omega L}{R_0} \left(1 - \frac{1}{L_0} \right) (-1 + i\omega \tau_{eff}) \right)^{-1}$$

With $L_0 = \frac{\alpha \cdot P}{G \cdot T}$ the electro-thermal loop gain and $\tau_{eff} = \tau_0 / L_0 - 1$

This equation shows one pole (fall time) at : $\tau_{fall} = \frac{C}{G} \frac{1}{1 + L_0 / (1 + \alpha_I)}$

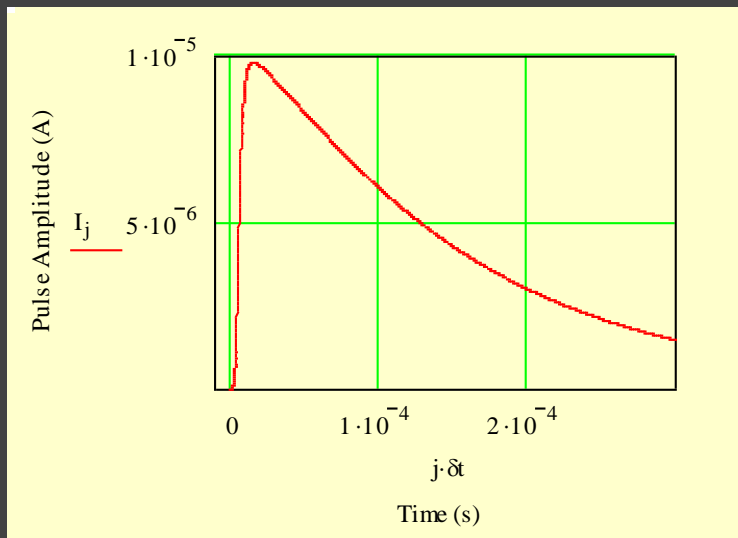
And a 2nd pole (rise time) at : $\tau_{el} = L / (R_{th} + R_0(1 + \alpha_I))$

Typical Micro-calorimeter Responsivity



$C = 0.5 \text{ pJ/K}$
 $G = 0.35 \text{ nW/K (P = 9 pW)}$
 $a_T = 100$
 $a^I = 1$
 $T = 0.1 \text{ K}$
 $L_0 \rightarrow 25$

$R_0 = 40 \text{ mOhm}$
 $R_{th} = 10.6 \text{ mOhm}$
 $L = 600 \text{ nH}$



1st pole 1.5 kHz/110 μs
(signal fall time)

2nd pole 24 kHz/6.7 μs
(signal rise time)

Matrix solution

$$\begin{bmatrix} \Delta I \\ \Delta T \end{bmatrix} \begin{bmatrix} i\omega L + R_{th} + R_0(1 + \alpha_I) & \frac{R_0 I_0}{T_0} \alpha_T \\ -R_0 I_0(2 + \alpha_I) & i\omega C + G - \frac{P_{J0} \alpha_T}{T_0} \end{bmatrix}^{-1} = \begin{bmatrix} V_{Johnson} + V_{noise} \\ -I_0 \cdot V_{Johnson} + P \end{bmatrix}$$

Thermal fluctuation noise

$$I_{Phonon} = P_{phonon} M_{INV}(0,1)$$

Johnson Noise

$$I_{Johnson} = V_{Johnson} [M_{INV}(0,0) - I_0 M_{INV}(0,1)]$$

Shunt noise

$$I_{shunt} = V_{noise} M_{INV}(0,0)$$

Micro-Calorimeter Noise sources

1) Phonon Noise

$$P_{Phonon} = \sqrt{4kT^2 G \Gamma}$$

in W/\sqrt{Hz} with $\Gamma \approx 0.5$

2) Johnson Noise

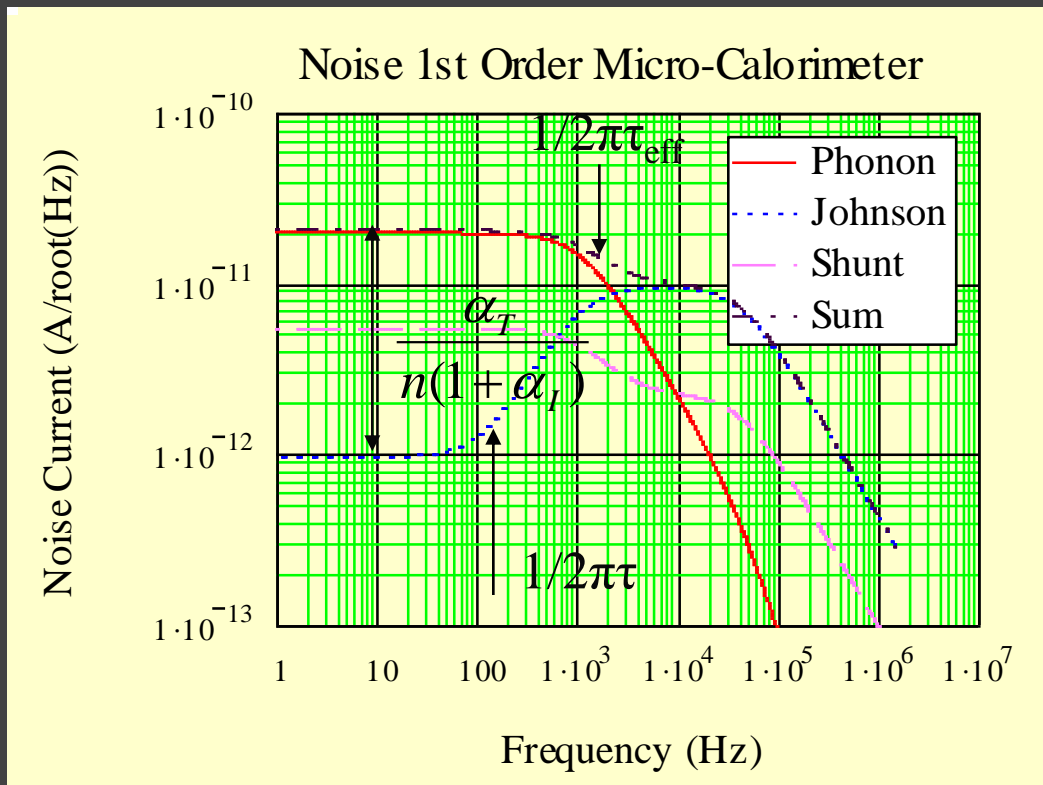
$$V_{Johnson} = \sqrt{4kTR\xi}$$

in V/\sqrt{Hz} with $\xi = 1 + 2\alpha_I$

3) Shunt noise

$$V_{shunt} = \sqrt{4kT_{sh} R_{sh}}$$

in V/\sqrt{Hz}

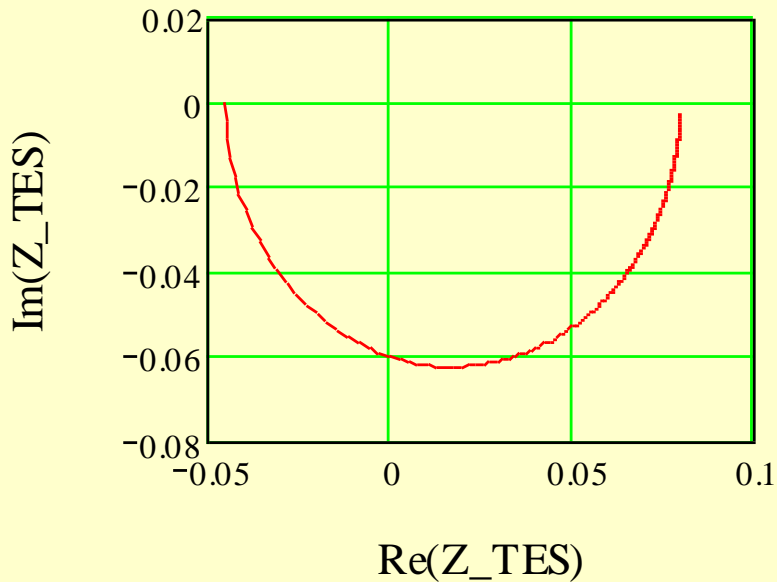


$$R_{sh} = 10.6 \text{ m}\Omega$$

$$T_{sh} = 60 \text{ mK}$$

Complex Impedance

$$Z_{TES} = M_{INV}^{-1}(0,0) - (R_{th} + i\omega L)$$



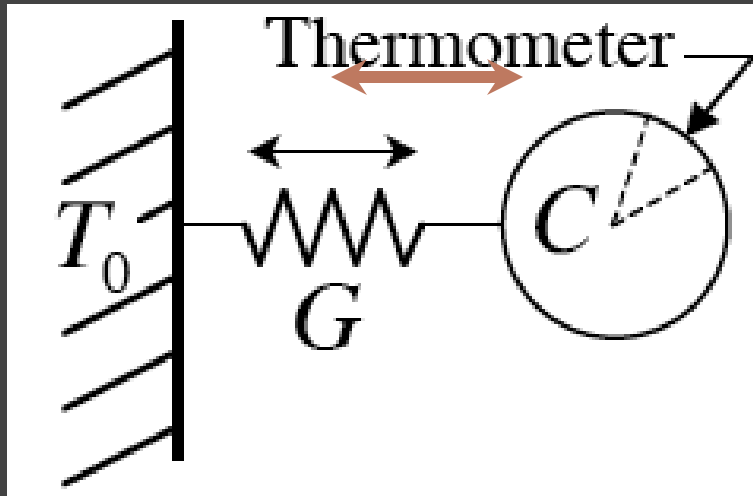
$$Z(0) = -R_0 \frac{1 + \alpha_I + L_0}{L_0 - 1}$$

$$Z(\infty) = R_0 (1 + \alpha_I)$$

$$\tau_{eff} = \frac{\tau_0}{L_0 - 1}$$

The effective time constant equals $1/\omega$ for the minimum imaginary number

Energy Resolution



Random transport of energy between heat sink and detector over thermal link G produces fluctuations in the energy content of C . The magnitude of these can easily be calculated from the fundamental assumption and definitions of statistical mechanics:

$$\sigma_E^2 = k T^2 C$$

“Thermodynamic Fluctuation Noise” (TFN)

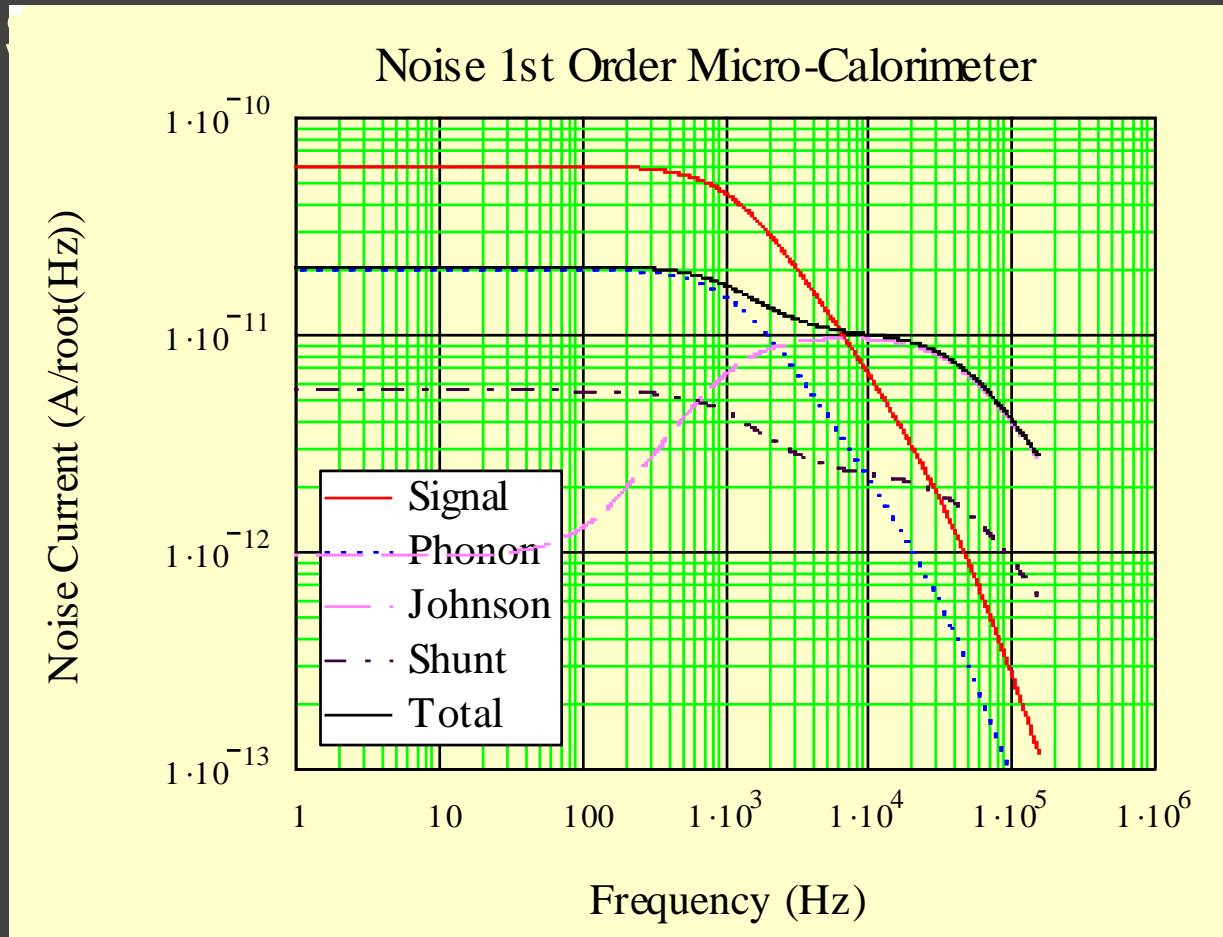
Can think of as Poisson fluctuations in number of energy carriers in C with mean c $N \approx \frac{CT}{kT}$, $\Delta E_{rms} = \sqrt{N} \cdot (kT) = \sqrt{kT^2 C}$.)

Not a limit on resolution, but sets the scale . . .

Energy Resolution

- Noise in different frequency bins uncorrelated
- Each frequency bin gives independent estimate of signal amplitude

• ∴



Energy Resolution in time domain

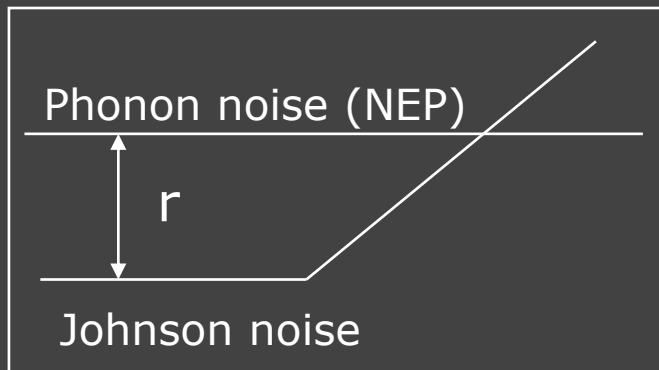
$$\Delta E = 2\sqrt{2\ln 2} NEP(0)\sqrt{\tau^*}$$

$1/2\pi\tau^*$ frequency where Johnson noise and TFN cross each other

$$NEP(0) = \sqrt{4kT^2G\Gamma}$$

with $\Gamma = 0.5$

Noise at input



$$\tau^* = \frac{C}{G r}$$

$$1/r = \sqrt{\frac{4kT/R}{4kT^2G\Gamma}} \frac{1}{L_{eff}} V \frac{1+L_{eff}}{L_{eff}} \approx \frac{1+\alpha_I}{\alpha_T} \sqrt{\frac{n(1+2\alpha_I)}{[1+(\frac{T_0}{T})^n]\Gamma}}$$

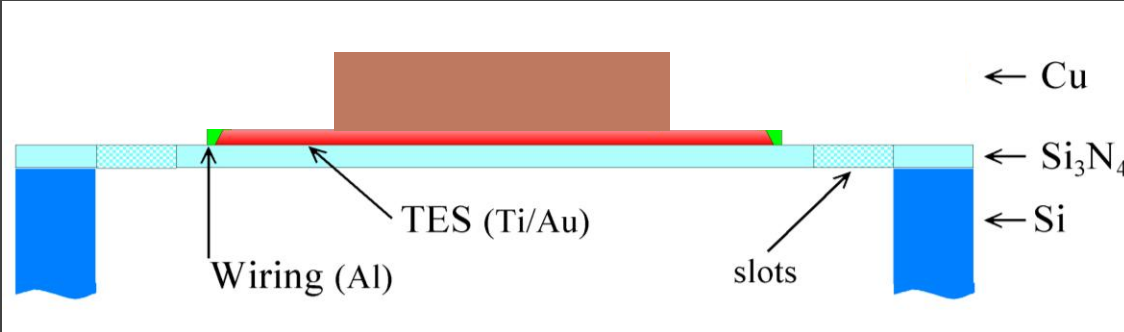
For $C = 0.5$ pJ/K, $n = 3$, $\alpha_T = 100$, $\alpha_I = 1$, and $T = 0.1$ K we get:
 $\Delta E = 1.64$ eV

Detector Characterization

Full Characterization includes:

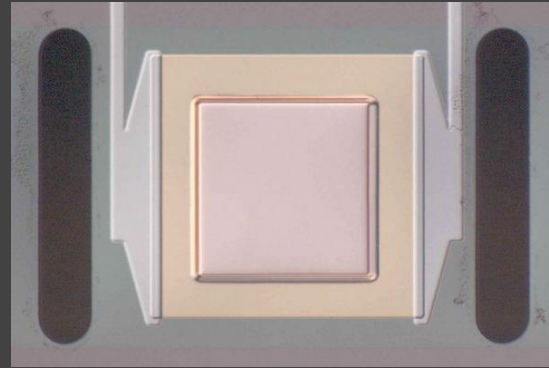
- RT measurements
- IV, $f(T_{\text{bath}}, \text{magnetic field})$
- Complex impedance
- Noise
- Baseline + X-ray energy resolution

Example: central Cu absorber

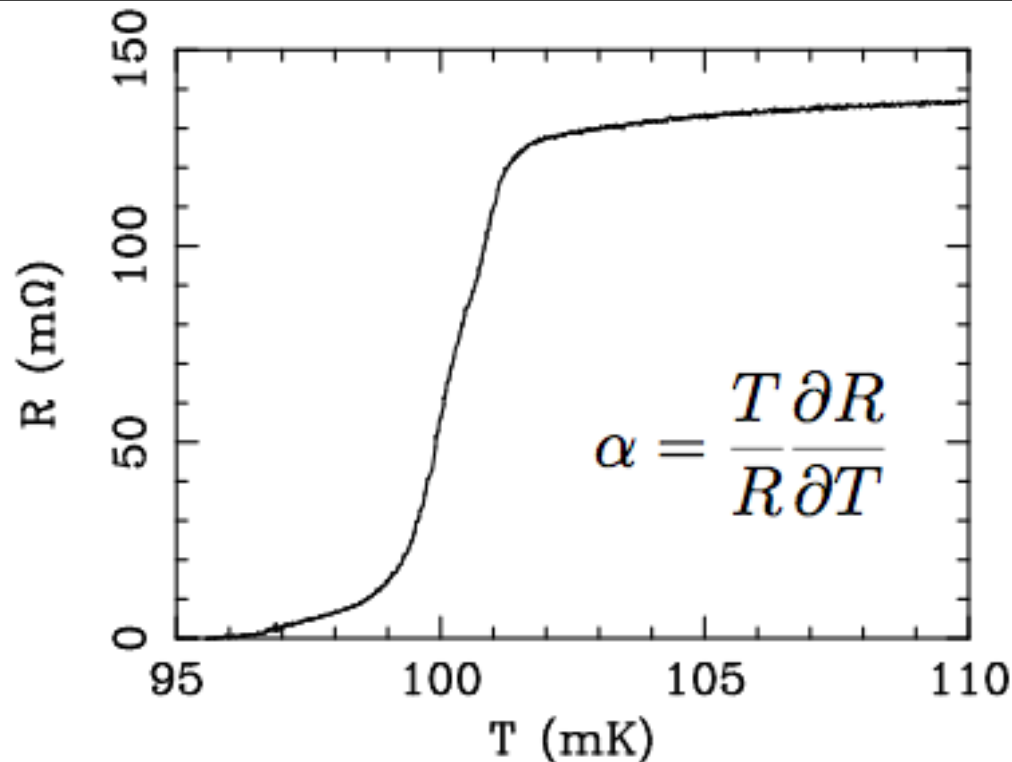


TES: TiAuTi
thickness: 20/50/5 nm
size: $146 \times 150 \mu\text{m}^2$

absorber: Cu
thickness: 1 μm
size: $100 \times 100 \mu\text{m}^2$



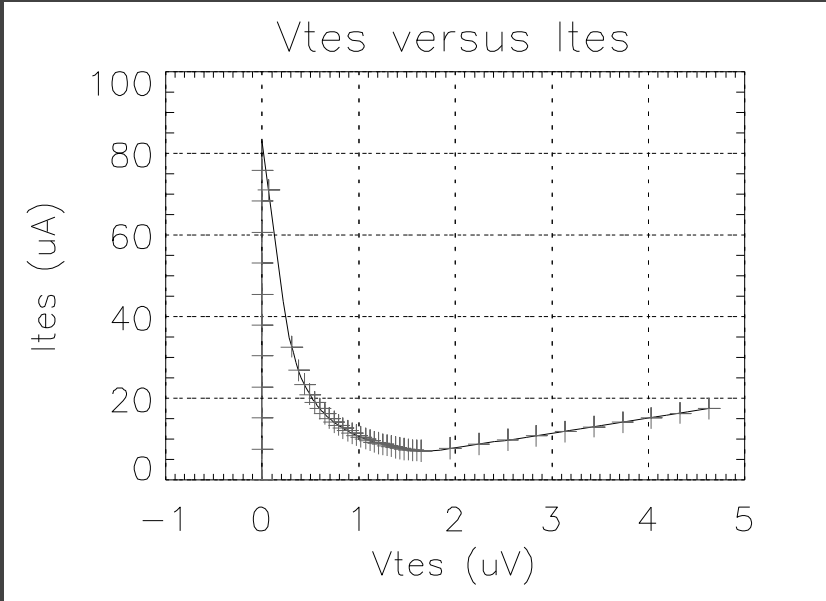
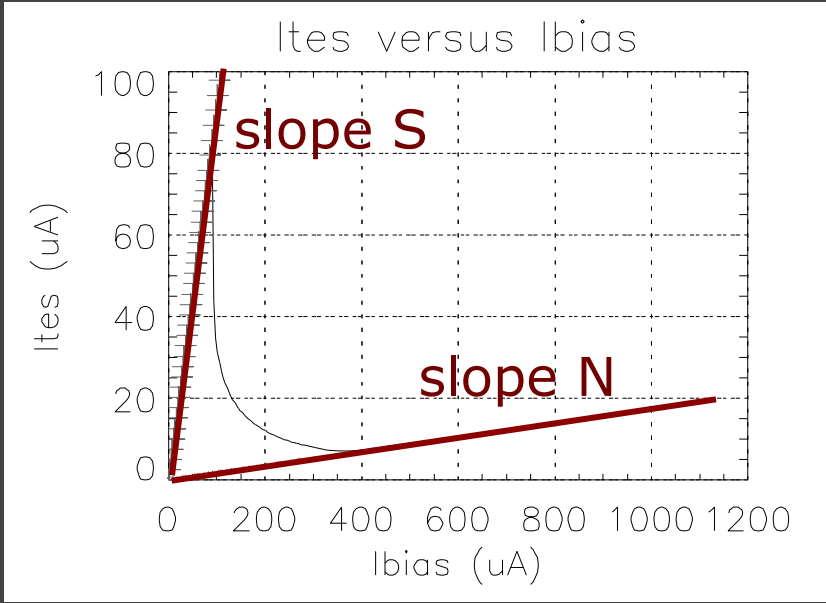
RT measurements



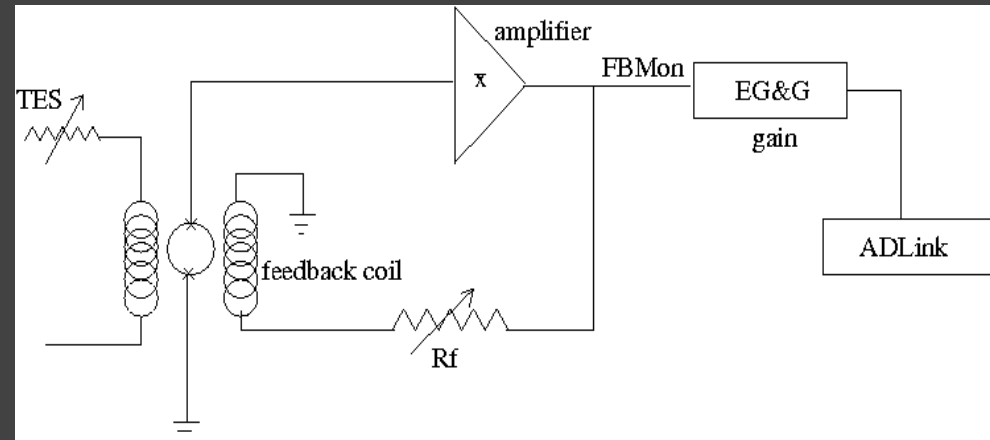
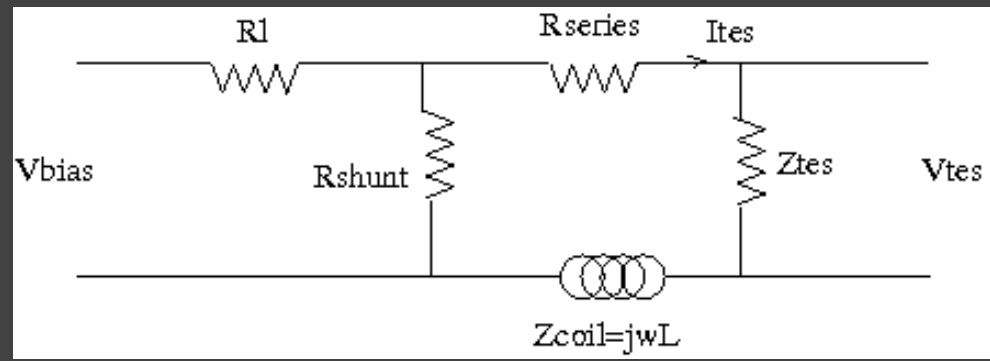
RT profile with small current

- Ti/Au bilayer with a Cu absorber
- $T_C = 100 \text{ mK}$
- $R_n = 143 \text{ m}\Omega$

IV measurements



Bias circuit



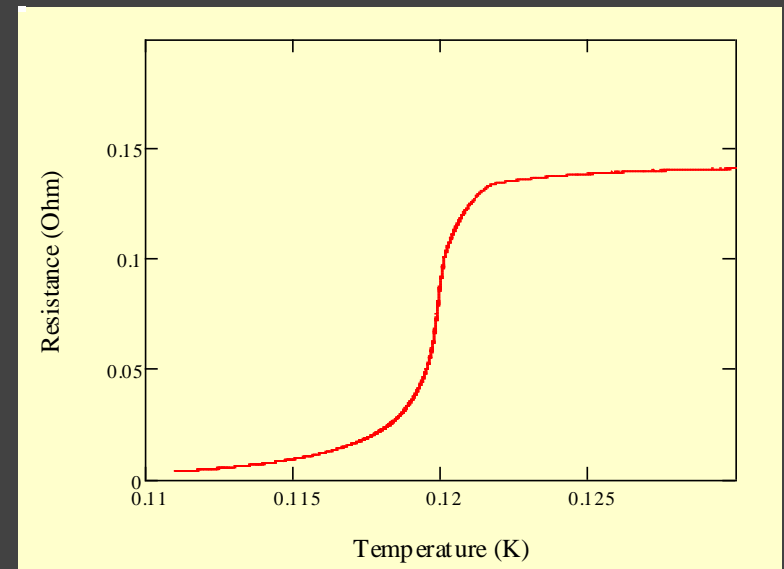
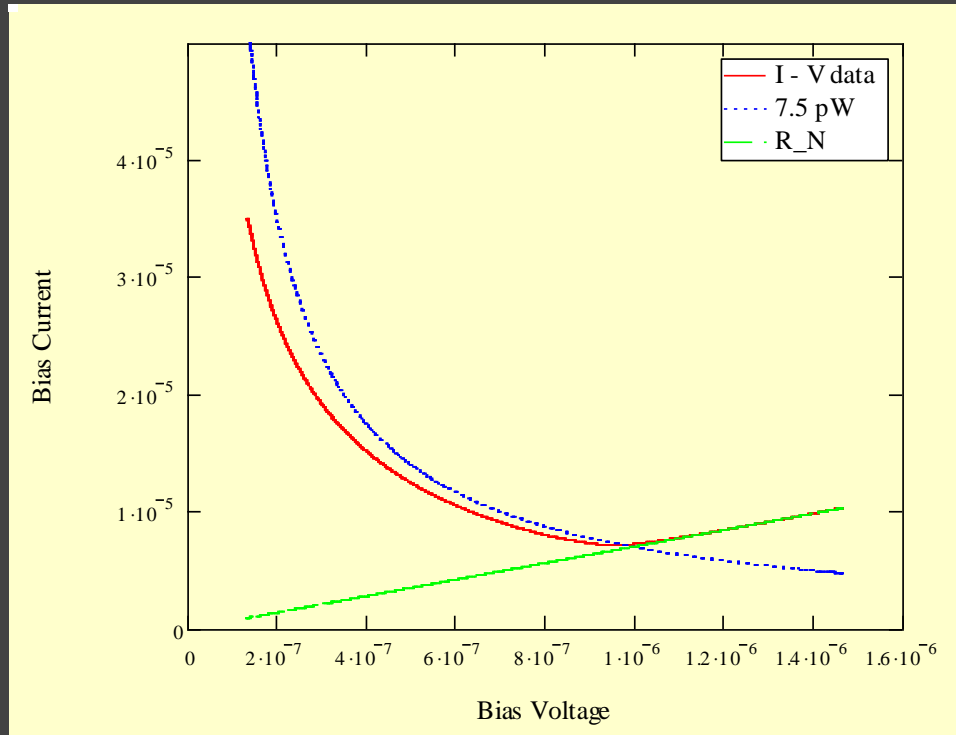
Read-out

P_{tes} (V)
 With n, T_C,
 → R(T) and

$$\alpha_{eff} = \frac{\alpha_T}{1 + \alpha_I / 2}$$

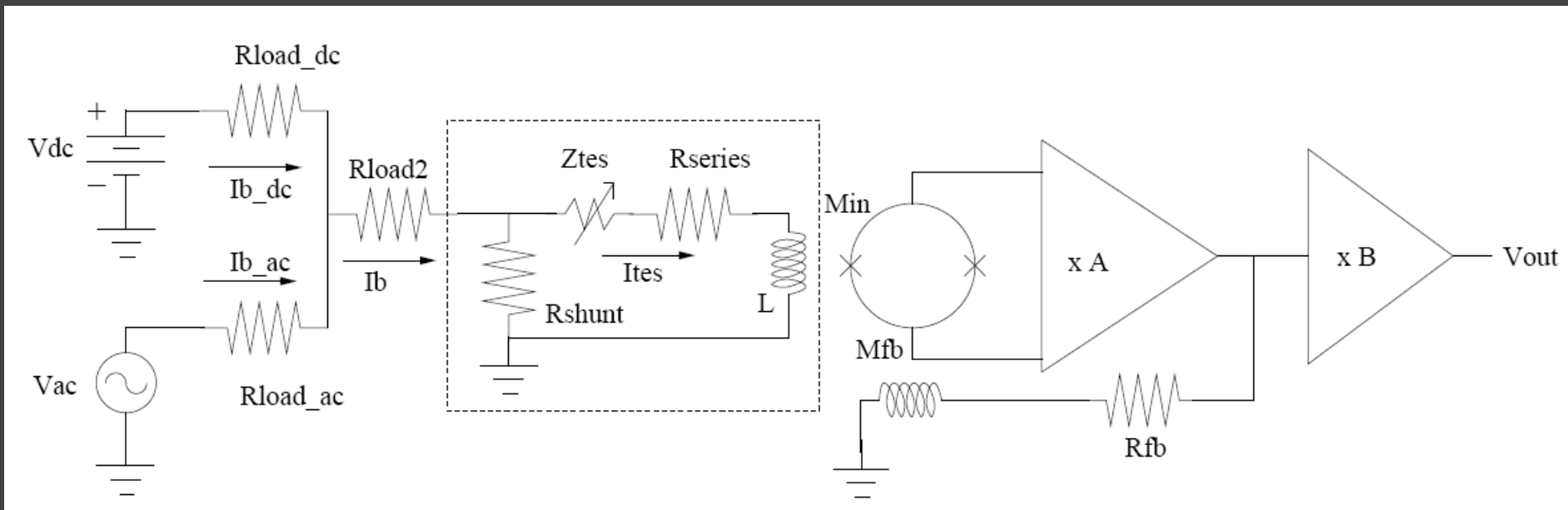
I - V Analysis

With knowledge of n (from P (T_{bath}) measurements, and T_C (From $R(T)$) we can derive the $R(T)$ from $I - V$, which is not equal to the $R(T)$ obtained by scanning in T with a constant measurement current



$$\alpha_{eff} = \frac{\alpha_T}{1 + \alpha_I / 2}$$

Complex impedance



Bias scheme with:

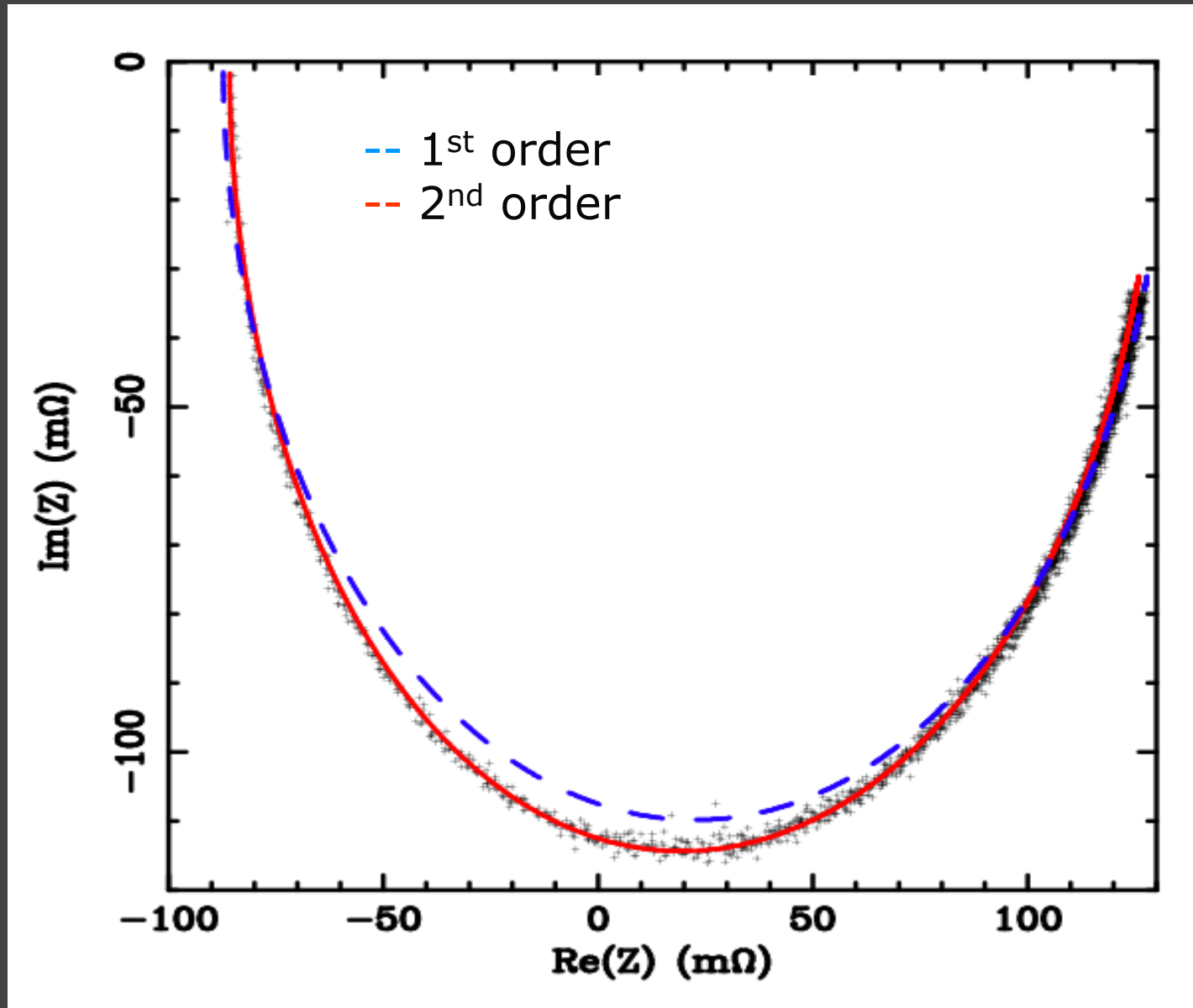
$$\bar{Z}_{TES}(j\omega) = \frac{\bar{V}_{AC}(j\omega)}{(R_{loadAC} + R_{load2})} \cdot \frac{R_{shunt}}{\bar{I}_{tes}(j\omega)} \bar{T}(j\omega) - \bar{Z}_{Th}(j\omega)$$

$$\bar{Z}_{Th}(j\omega) = R_{series} + R_{shunt} + j\omega L$$

\$T(j\omega)\$: transfer function of the signal lines → determined experimentally

\$Z_{normal}/Z_{super}\$ gives \$L\$, then \$Z_{super}\$ leads to determination of \$T(j\omega)\$

Complex impedance

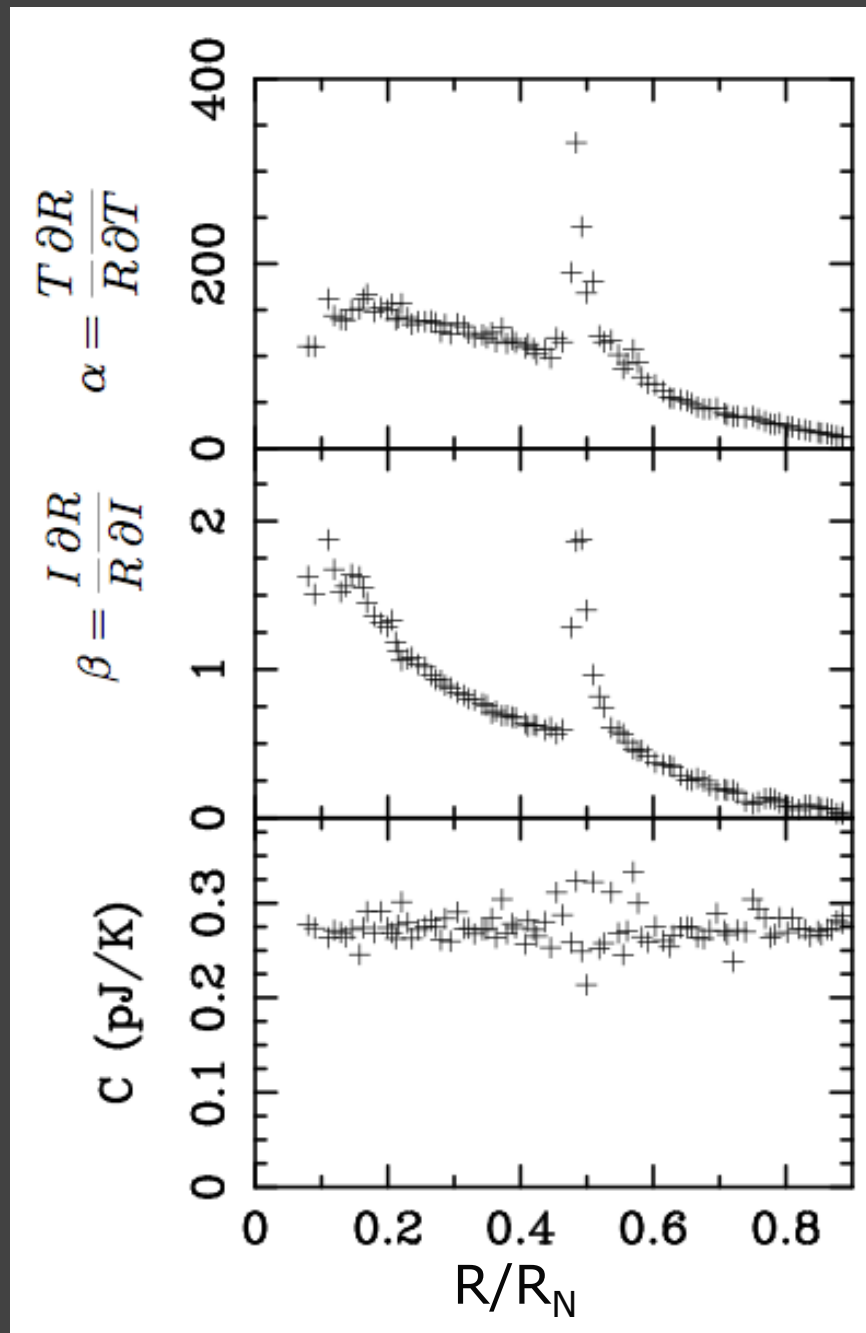


Complex impedance

2nd order due to “dangling”
heat capacity with:

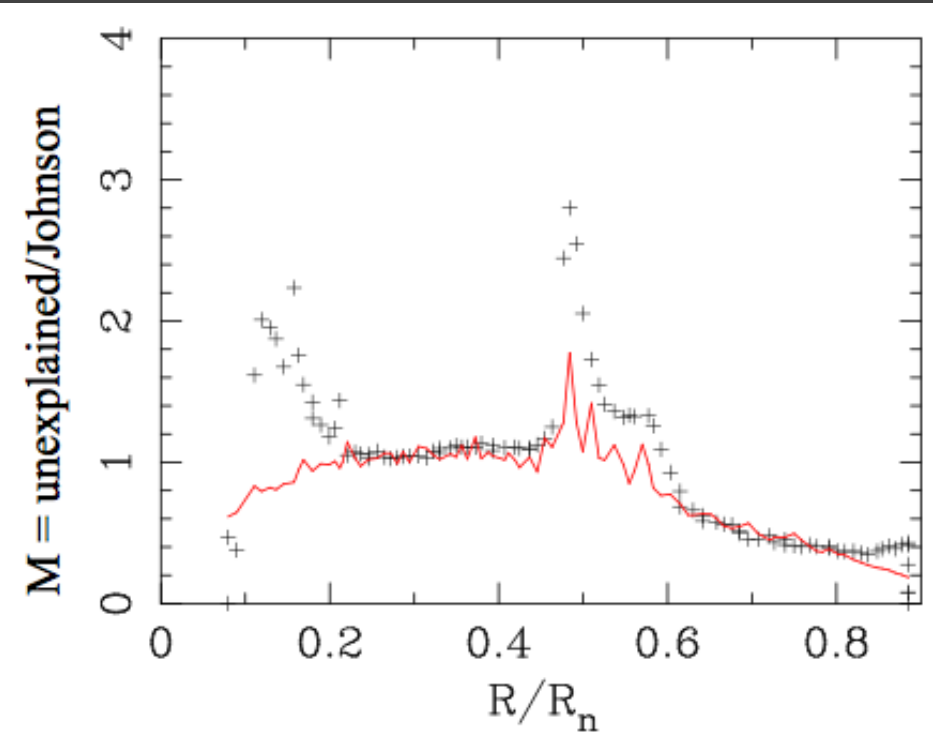
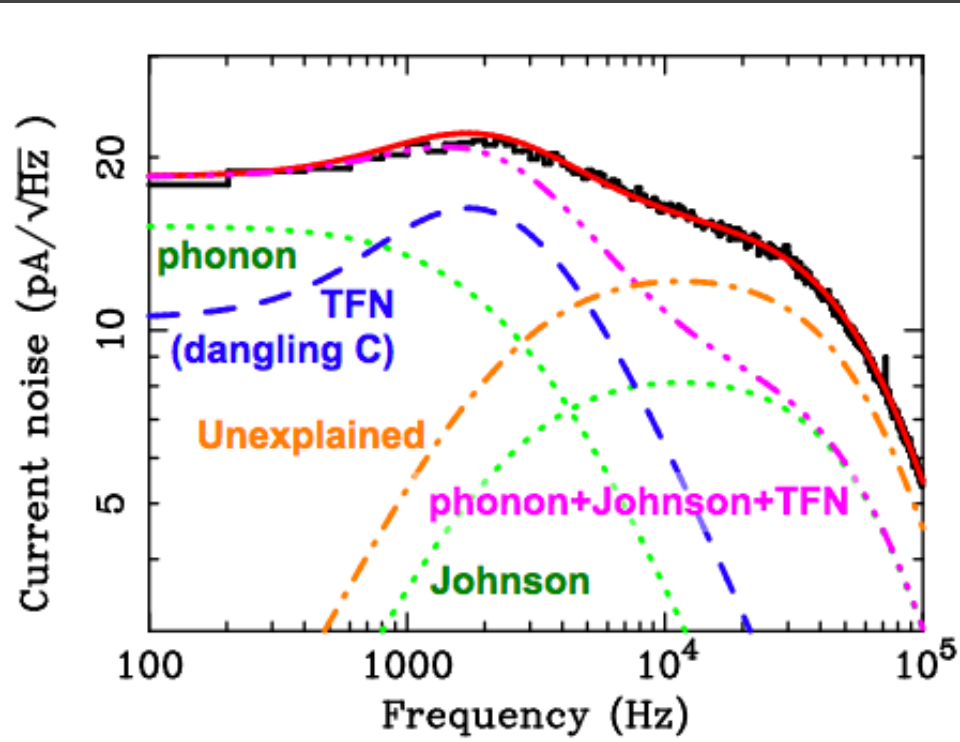
$$C_D = 0.04 \text{ pJ/K}$$

$$G_D = 0.4 \text{ nW/k } (\tau_D = 0.1 \text{ ms})$$



Noise (Measurement and Model)

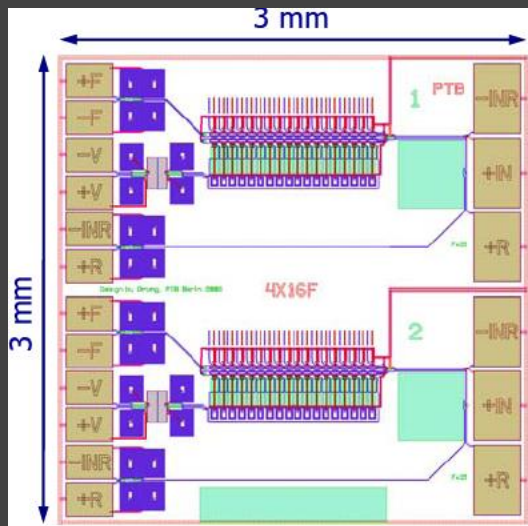
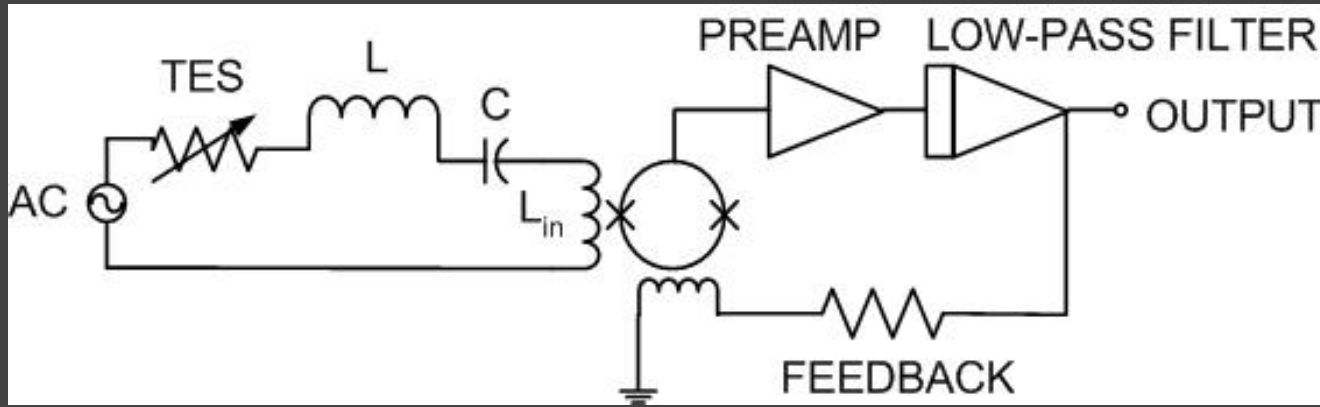
variables from complex impedance
used to fit noise spectra:



Read-out Electronics

- 1) SQUID-amplifier
- 2) Multiplexing
 - 1) Introduction
 - 2) FDM
 - 3) (Baseband) Feedback
 - 1) Principle
 - 2) Characteristics
 - 3) Implementation
- 3) LC-filters

TES READ-OUT BY SQUID AMPLIFIER



PTB 16-SQUID-arrays

Typical SQUID parameters:

- $L_{in} = 3 \text{ nH}$
- $\Phi_n = 0.22 \mu\Phi_0/\sqrt{\text{Hz}}$
- $i_N = 5 \text{ pA}/\sqrt{\text{Hz}}$
- Dyn.Range +/- 0.45 $10^6 \sqrt{\text{Hz}}$

Signal Characteristics:

$$i_{\text{Johnson}} = \sqrt{4kT/R} = 12 \text{ pA}/\sqrt{\text{Hz}}$$

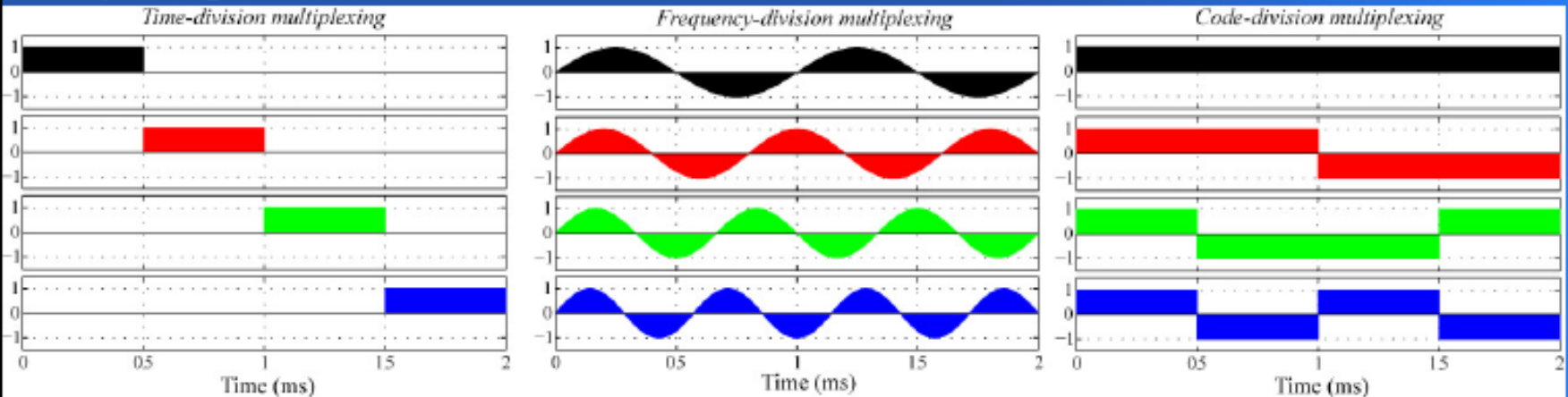
$$\text{Dyn.Range} = \frac{E_{\text{max}}}{\Delta E_{\text{rms}} \sqrt{\tau}} = \pm 10^6 \sqrt{\text{Hz}}$$

Noise levels ok

SQUID dynamic range $\approx 6x$ too small \rightarrow feedback required for dynamic range and linearization

Multiplexing

Multiplexing basis sets



Time-division (e.g. TDMA cell phones)

- Classic SQUID multiplexer circuits that switch by turning on SQUIDs (or shunting with flux-actuated switches).

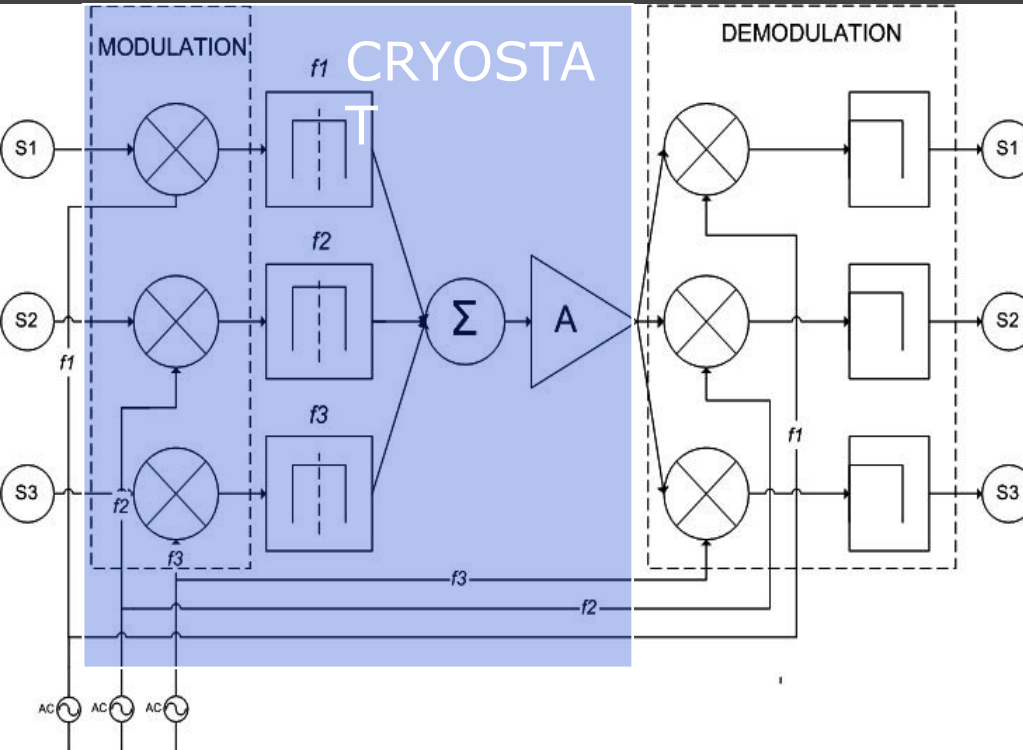
Frequency-division (e.g. FDMA cell phones)

- Under development in SRON and Japan

Code-division (e.g. CDMA cell phones)

1. Uses same room-temperature electronics as TDM ("TDM Turbo")
2. Only one SQUID per column
3. Ultra-low-power switches modulate polarity of coupling
4. Detectors dc biased
5. No multiplex disadvantage

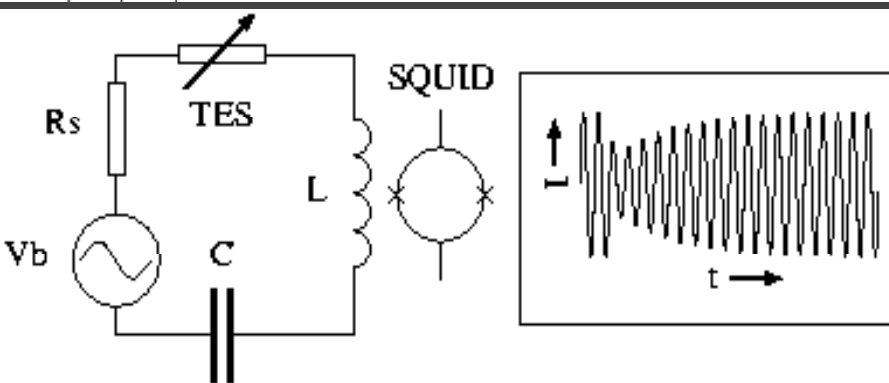
FREQUENCY-DOMAIN-MULTIPLEXING



1 column or row of pixel-array shown as example

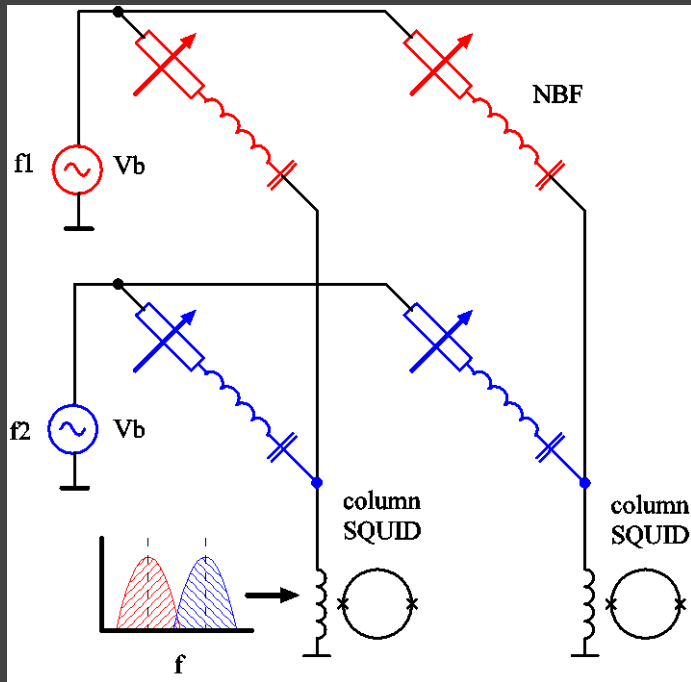
FDM operation:

- TESs act as AM-modulators
- TESs AC-biased at frequencies f_1, f_2, f_3, \dots
- Each TES equipped with LC band pass filter around carrier frequency to block wide-band noise
- Summed signal read-out by one SQUID-amplifier per column
- Demodulation by amplification and filtering



FREQUENCY DOMAIN MULTIPLEXING

Design Issues



- 1) Summing topology
- 2) Chosen for current summing
- 3) Feedback required to minimize common impedance, linearize SQUID response, and increase dynamic range
- 4) LC-filter inductance set by TES stability requirements. Critical damping sets $L \approx 1 \mu\text{H}$, for $R = 40 \text{ m}\Omega$ and $\alpha_I = 1$

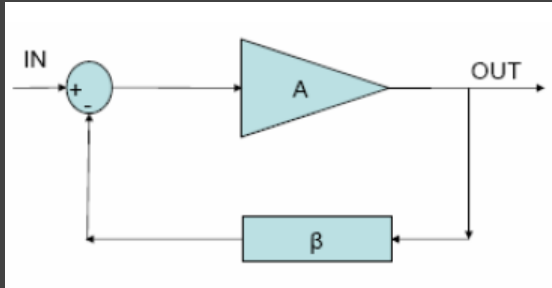
$$L/R = \frac{1}{2}(3 + \alpha_I - 2\sqrt{2 + \alpha_I})\tau_{\text{eff}}$$

$$R_{\text{ESR}} = \frac{\omega L}{Q} < R_{\text{sh}}$$

$$\omega = \frac{R}{k_c^2 L_{\text{in}}}$$

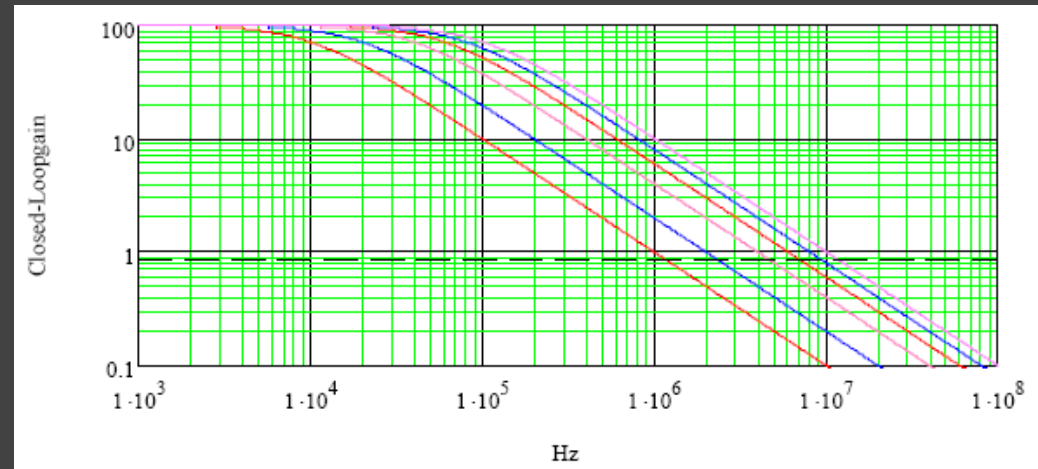
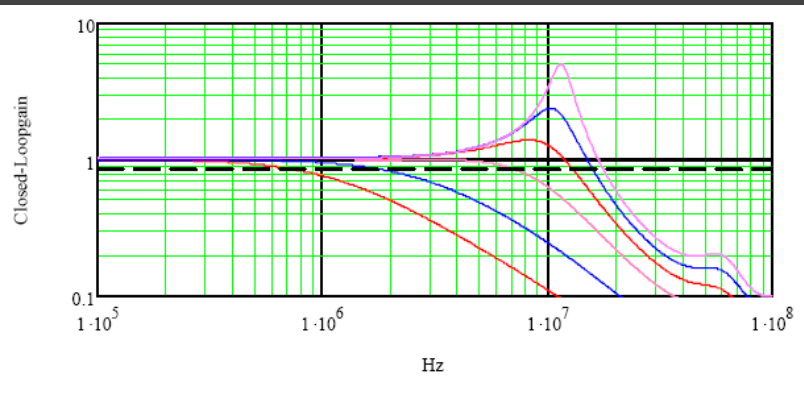
- 5) 1 – 10 MHz frequency range
 > 1 MHz LC-filter capacitance large at low f
 < 10 MHz due to SQUID back action noise ($L_{\text{in}} < 0.6 \text{ nH}$ for $k_c = 1$), and LC-filter losses ($Q > 10.000$)
- 6) Frequency spacing (> 50 kHz to keep crosstalk low)

Standard FLL limitations



$$f_{1,\max} = \frac{1}{4\pi t_d} = 0.08 / t_d$$

Delay in FLL seriously limits the available bandwidth



Closed loop response for $\beta=1$ and for $\beta = 0.01$ and a 20 ns delay
 Resulting in a maximum stable $f_1 = 8$ MHz. So for 6x loopgain
 only a bandwidth of 1.3 MHz is available

Baseband feedback

Use the fact that:

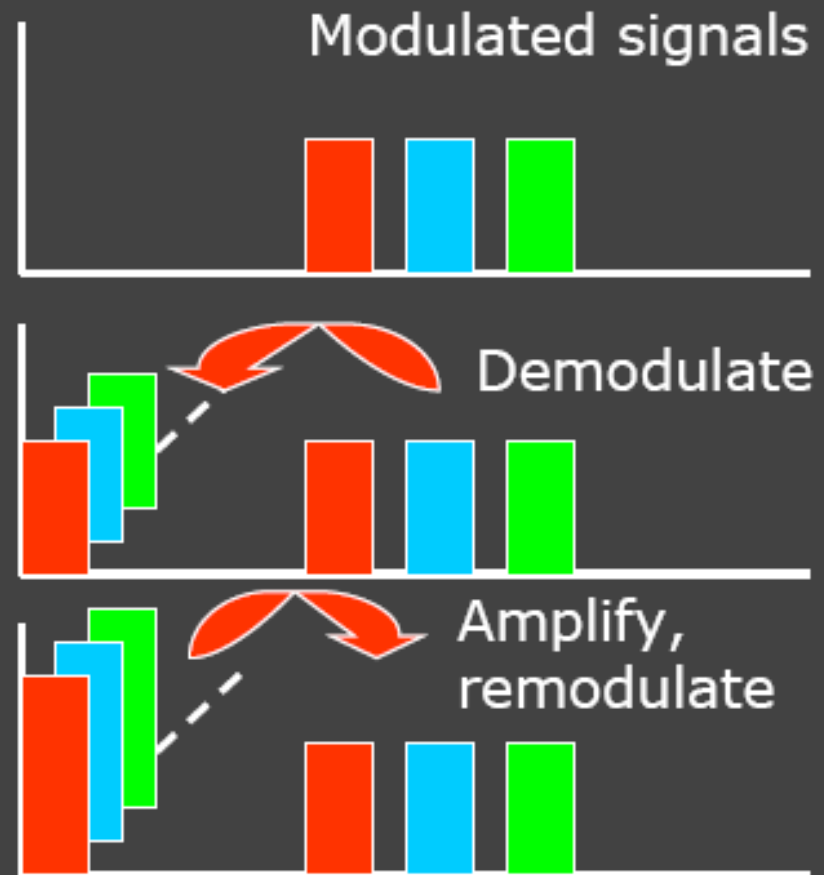
- Only the envelope contains information
- The carrier is deterministic

⇒ Feedback on envelope only

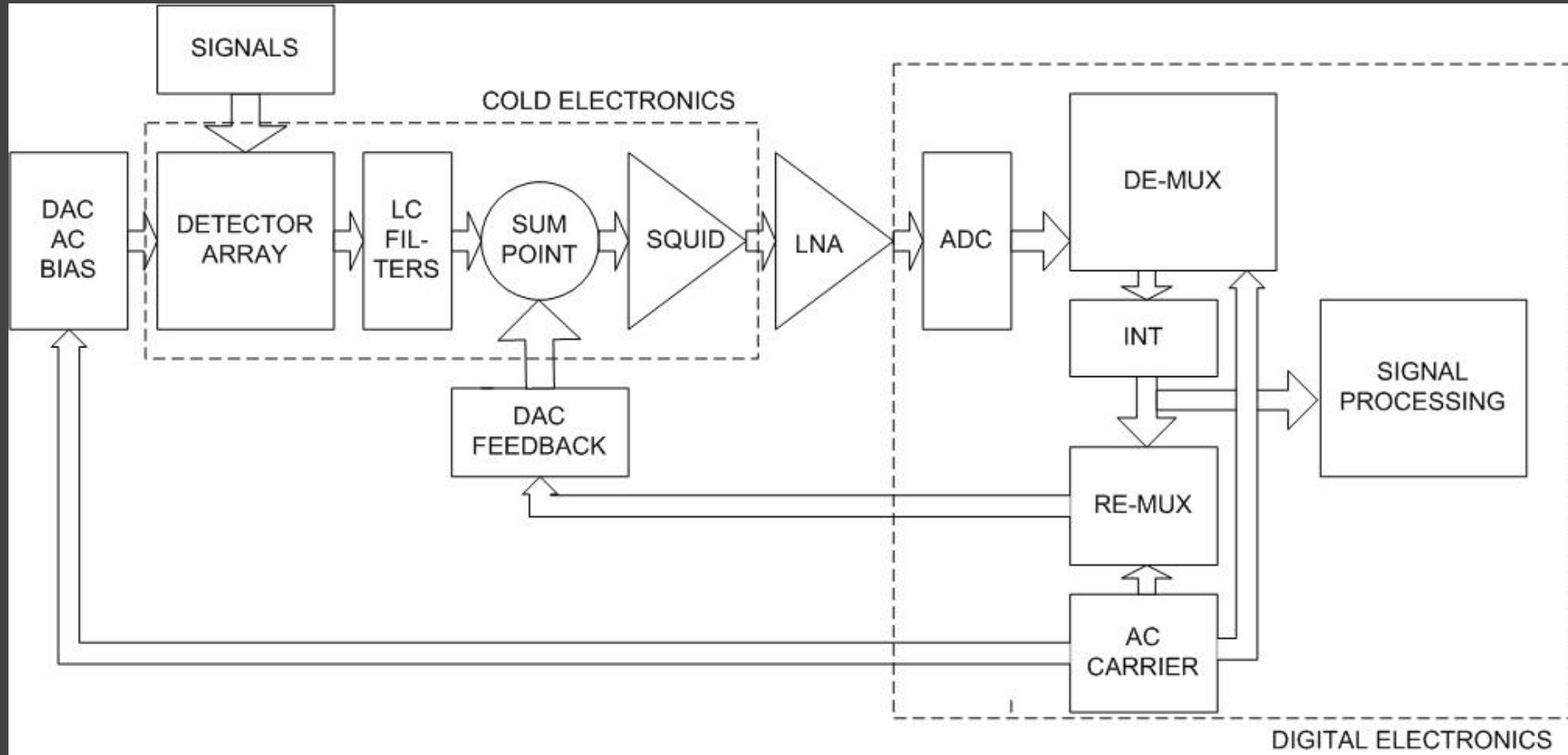
⇒ One channel per pixel

⇒ Maximum GBW set by channel separation ($GBW \approx \Delta f/6$)

⇒ Very similar to the frame rate limitation in TDM on GBW



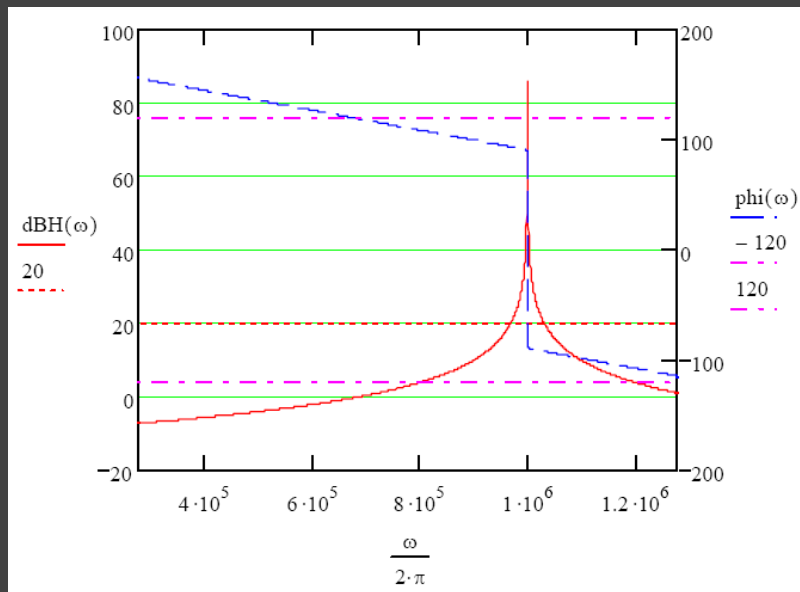
Baseband feedback implementation



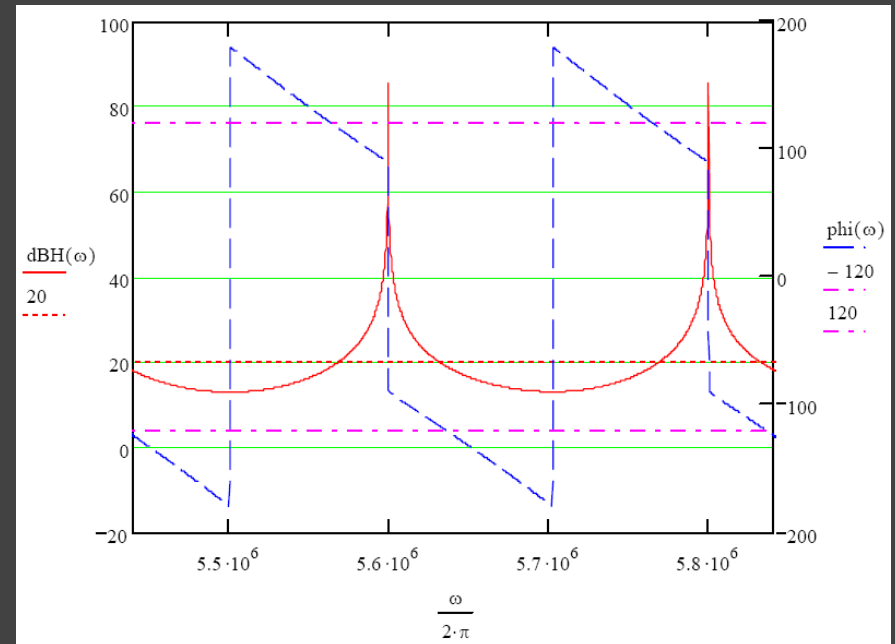
Baseband Feedback Filter characteristics

$$H(\omega) = \frac{e^{-j(\omega T_d - \varphi)}}{1 + j(\omega - \omega_c)\tau}$$

The transfer function around each carrier frequency consists of an integrator, a delay term and a phase compensation of the delay



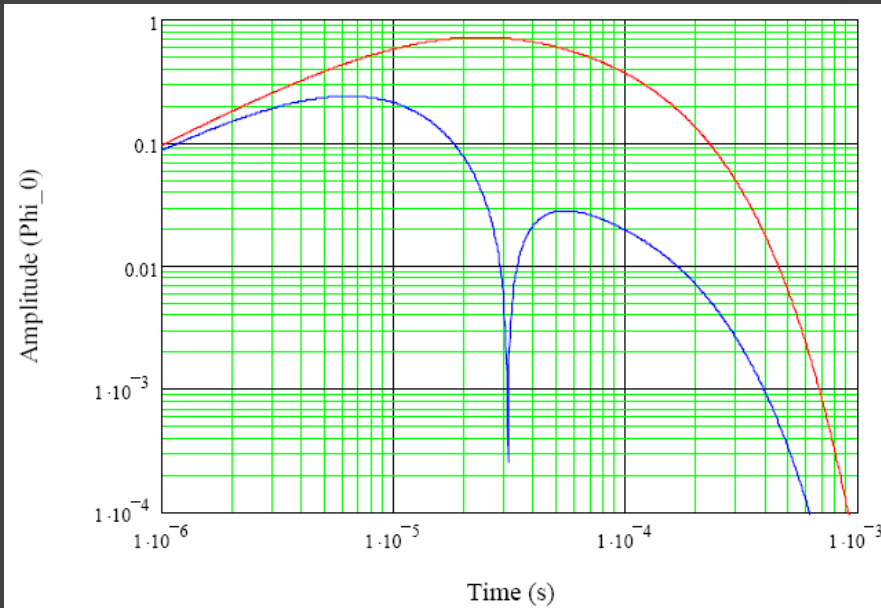
Amplitude and phase for a single Carrier (250 ns delay)



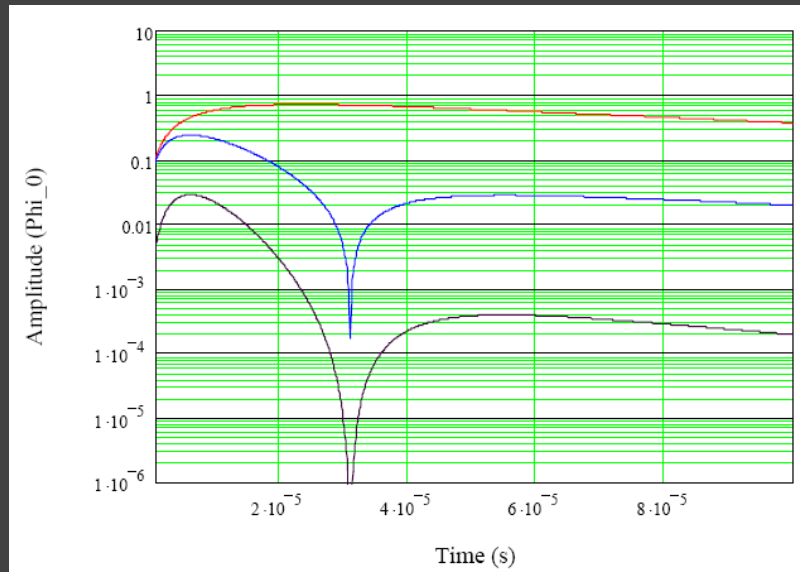
Amplitude and phase of two central carriers out of 32

For a 60° phase margin the Gain-bandwidth around each carrier is limited to about $\Delta f/6$, i.e. 33 kHz for 200 kHz carrier separation

Simulations on error signal and 2nd harmonic



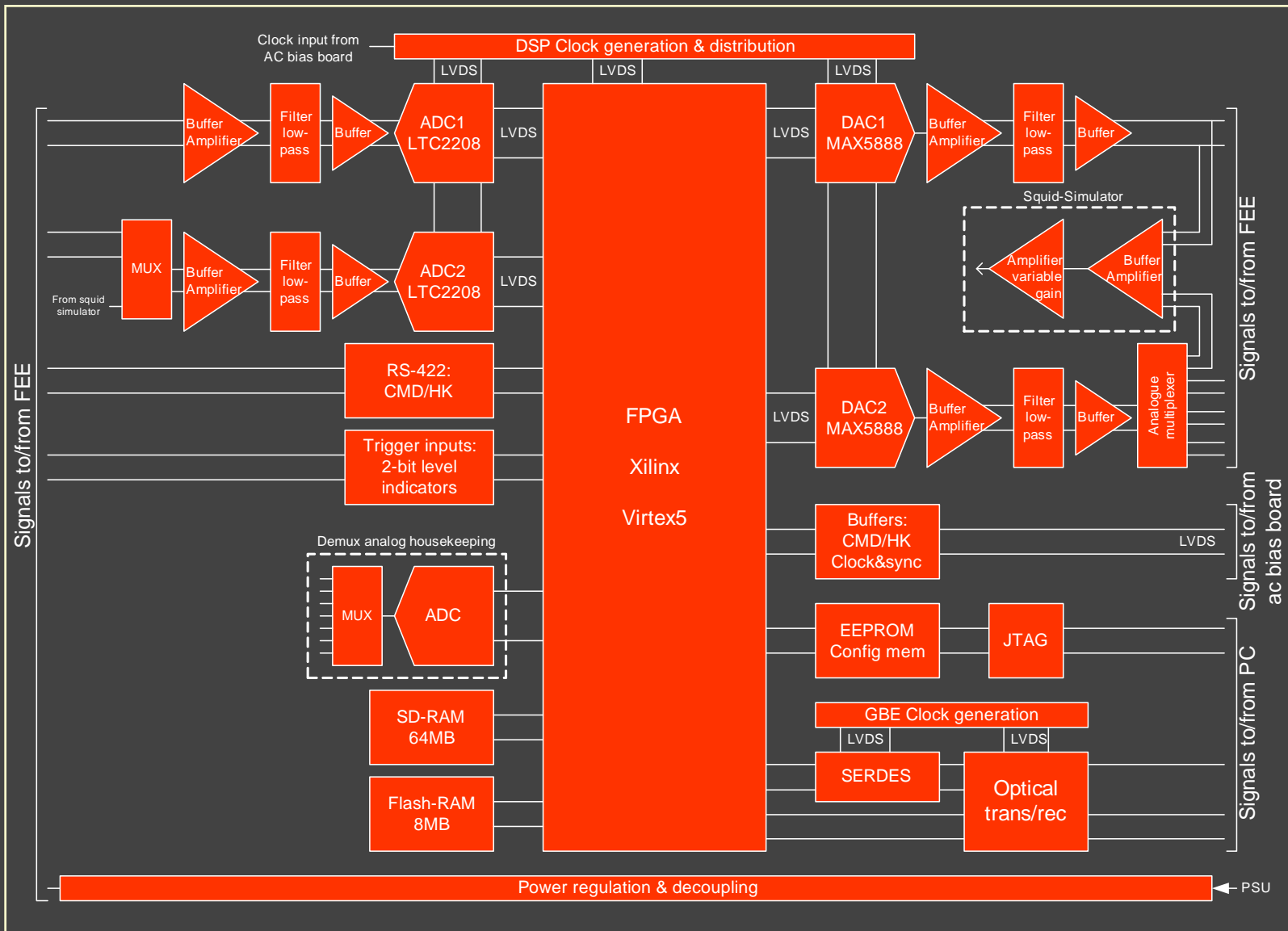
- Signal amplitude of 1 Φ_0 (0.2 $\mu\Phi_0/\sqrt{\text{Hz}}$ noise and $\pm 5 \cdot 10^6 \sqrt{\text{Hz}}$ dyn. Range)
- Signal with 10 μs risetime and 100 μs falltime
- Blue error signal at SQUID input for BBFB with a GBW = 32 kHz
 - error signal amplitude scales with $1/T_{\text{rise}}$



Linear time axis showing also the 2nd order harmonic for $k_2/k_1 = 1$

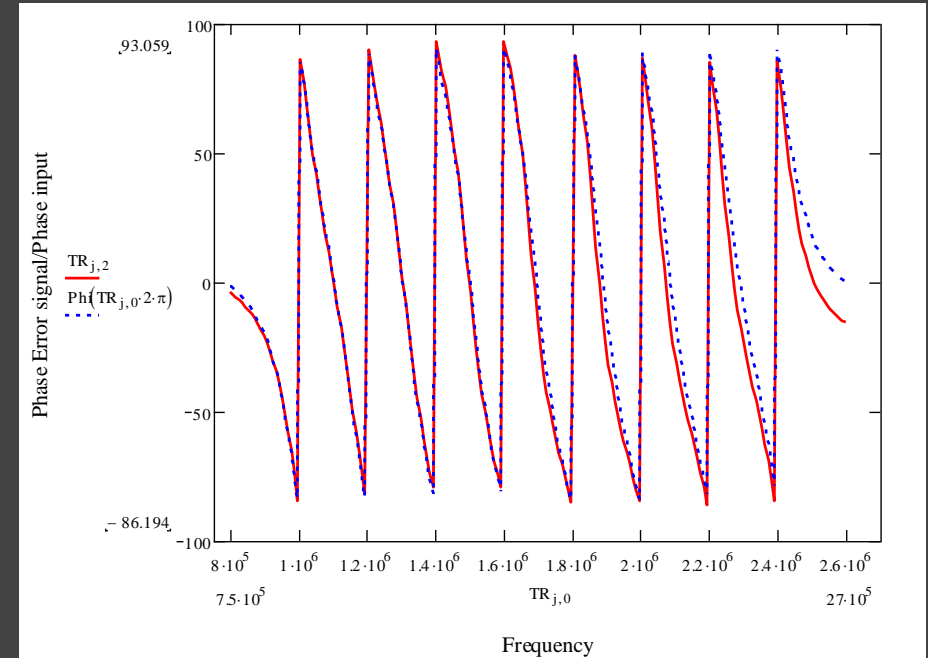
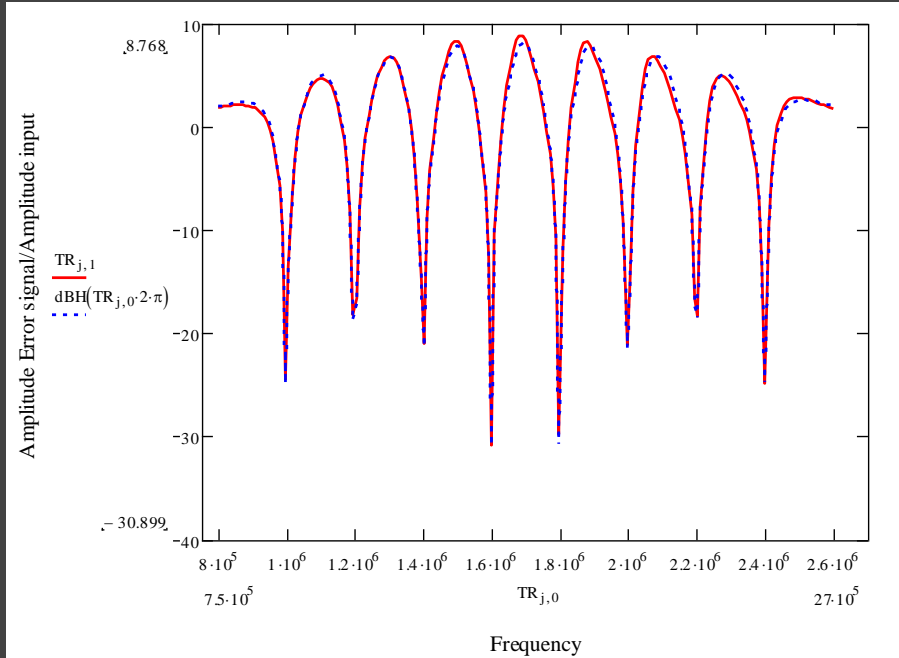
The 2nd order contribution in this case equals $7 \cdot 10^{-3}$

BaseBand Feedback Electronics board



Amplitude and Phase (error signal/input signal) for 8 channels with BBFB

Red lines: Data from a commercial Xylinx breadboard
Blue lines: Model



Amplitude: red-data blue-model Phase: red-data blue-model

Gain-bandwidth of 35 kHz for 200 kHz spacing and 830 ns delay

FLL-gain of 2x at highest signal frequency (16 kHz)

2. Measurements

- 4. TP generated by DeMux board; TES normal
367 kHz carrier generated by DeMUX board
Baseband feedback by DeMux board
Digitization and demodulation via DeMUX board

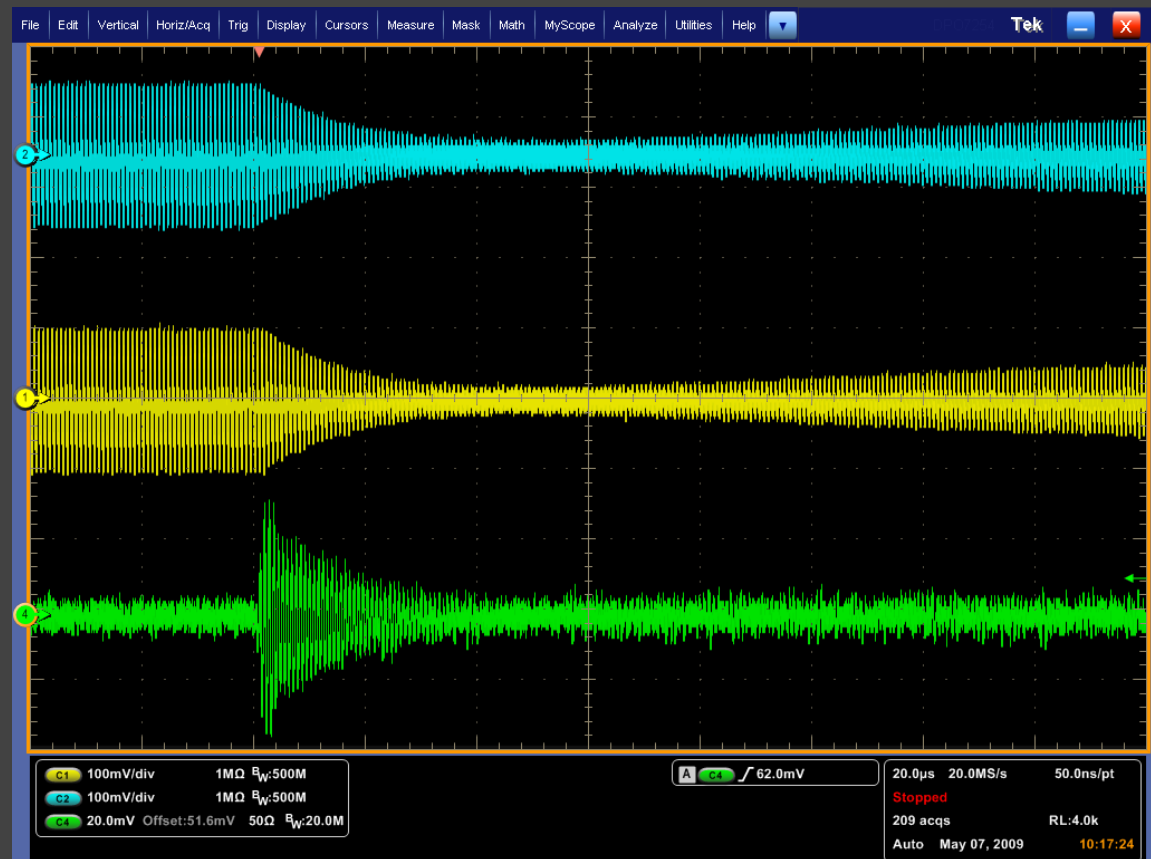
Closure demonstrated
at 367 kHz and 1 MHz

Loop gain = 18
GBW = 300 kHz

Carrier + tailpulse

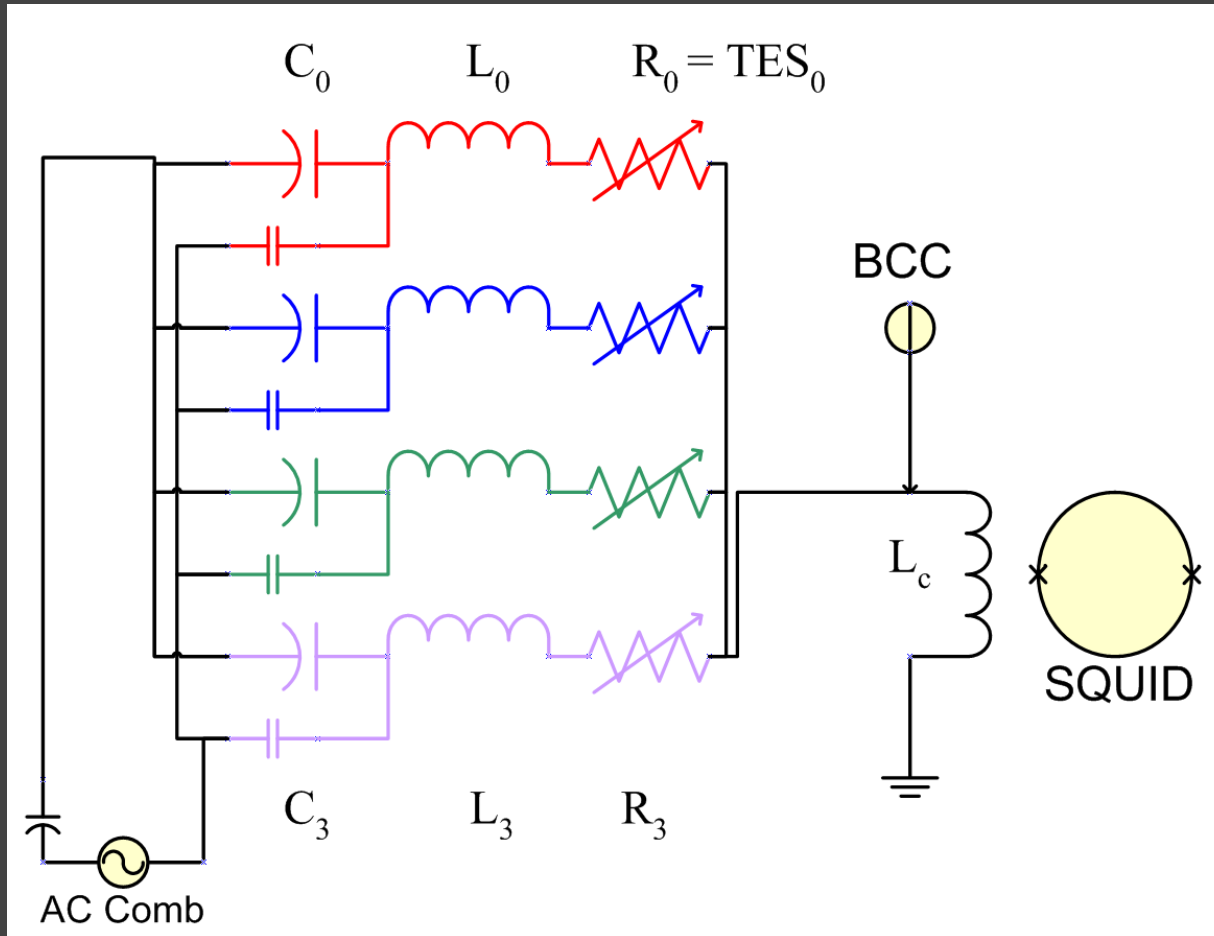
Feedback signal
(de- & remodulated)

Error signal x 25



LC-filters

circuit & implementation



LC-filters

circuit & implementation

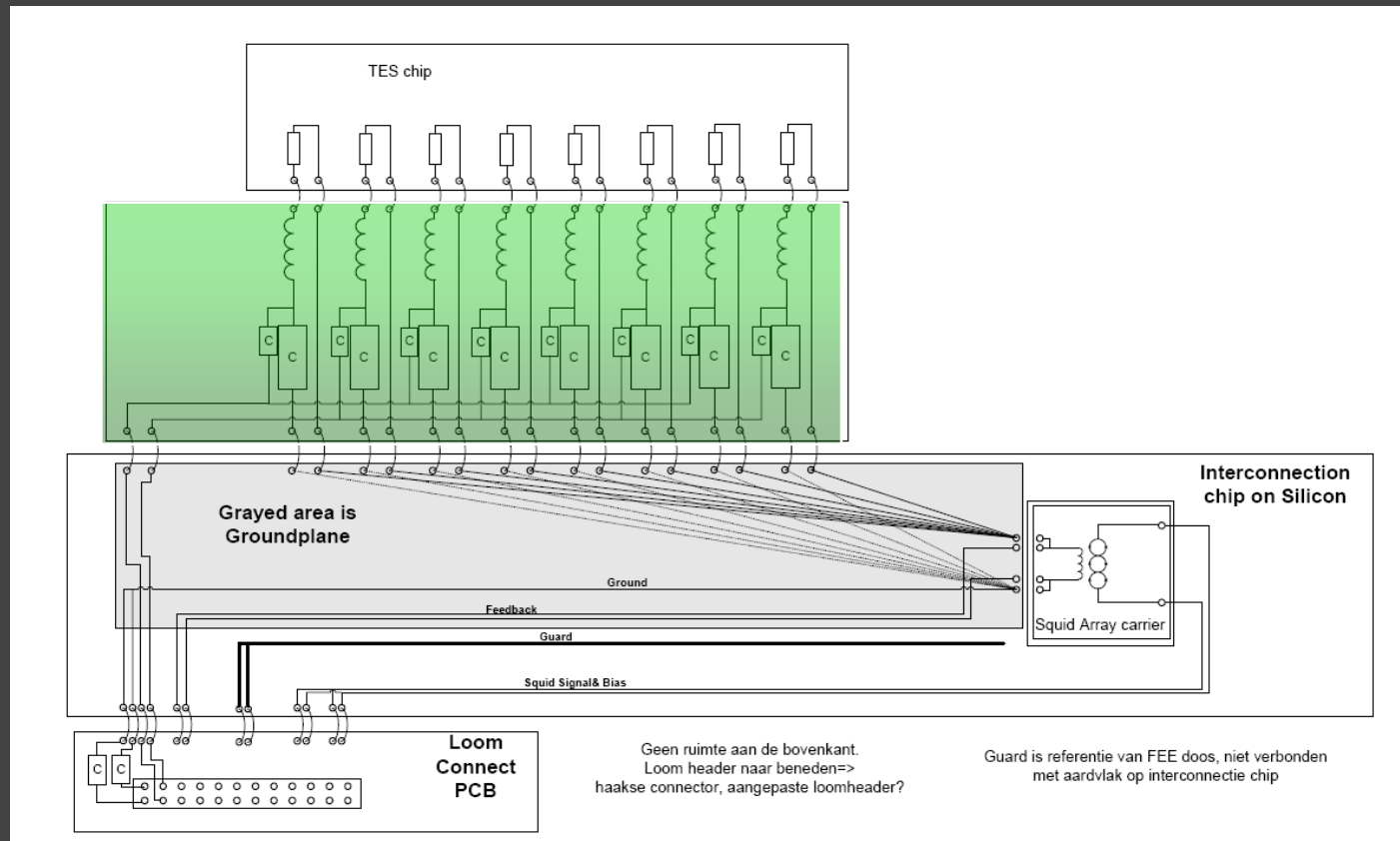
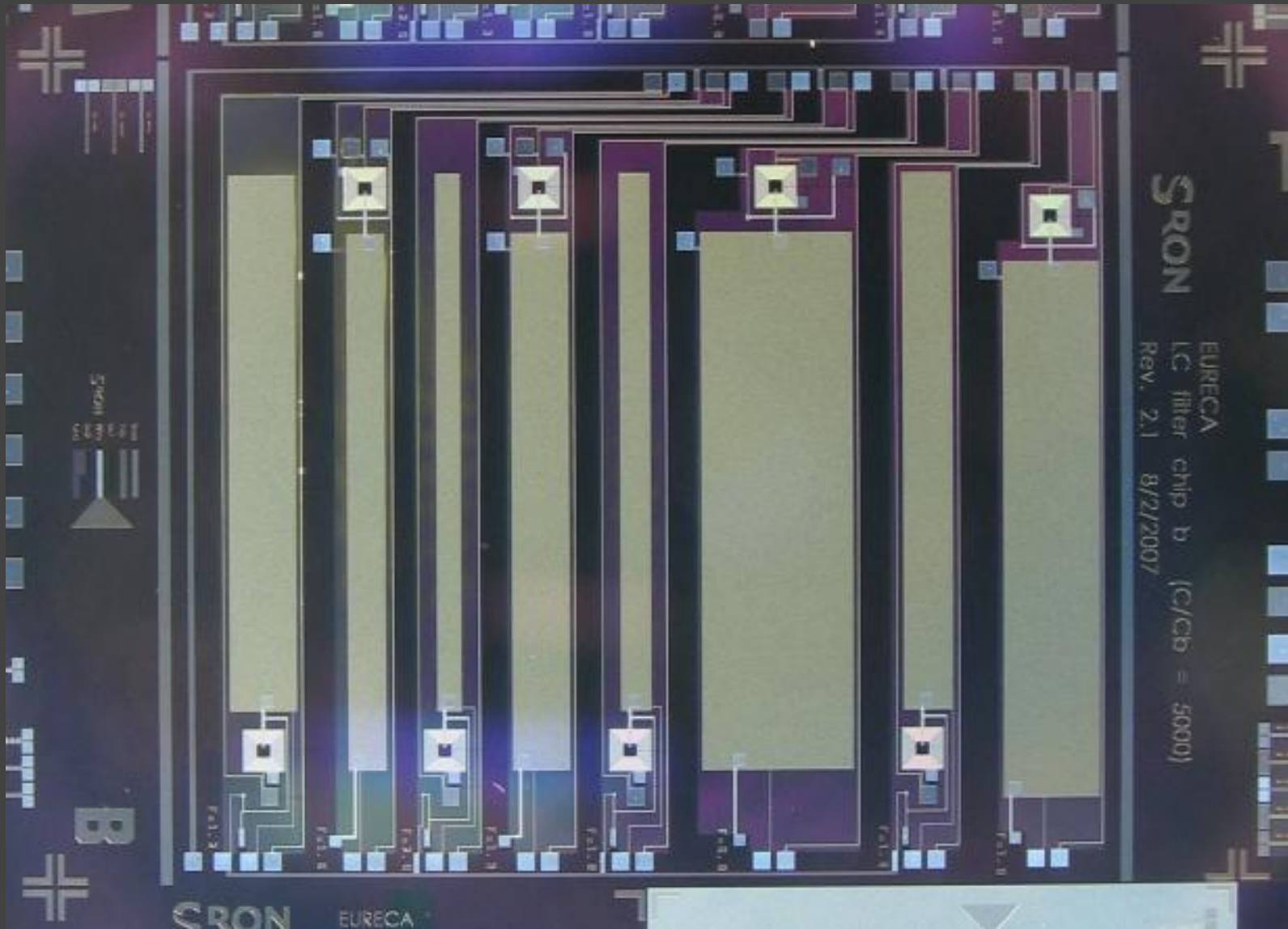


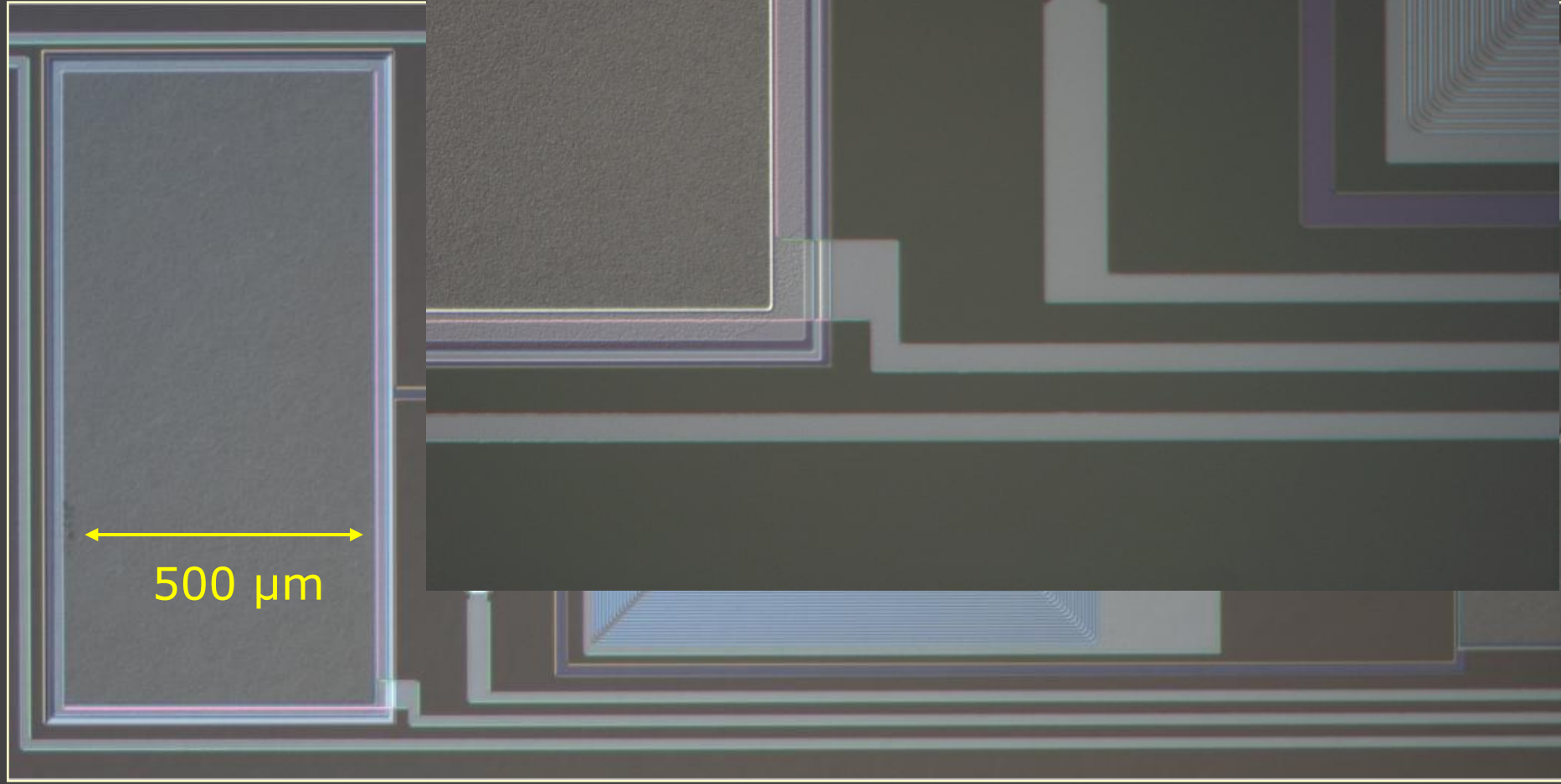
Figure 2. Electrical scheme for the bias and signal chain of the first Eureka channel. The components for each TES chain are laid-out in parallel lanes as much as possible.

8 channel LC chip design



20 x 14 mm²

LC filterchip

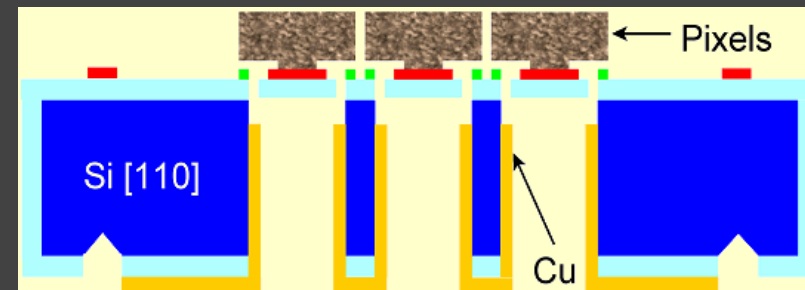
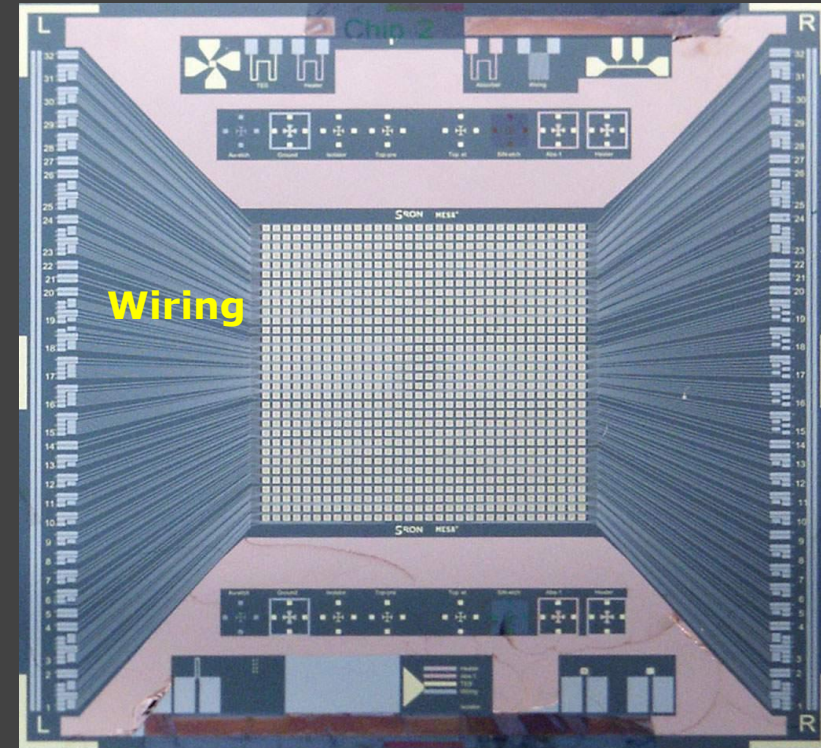
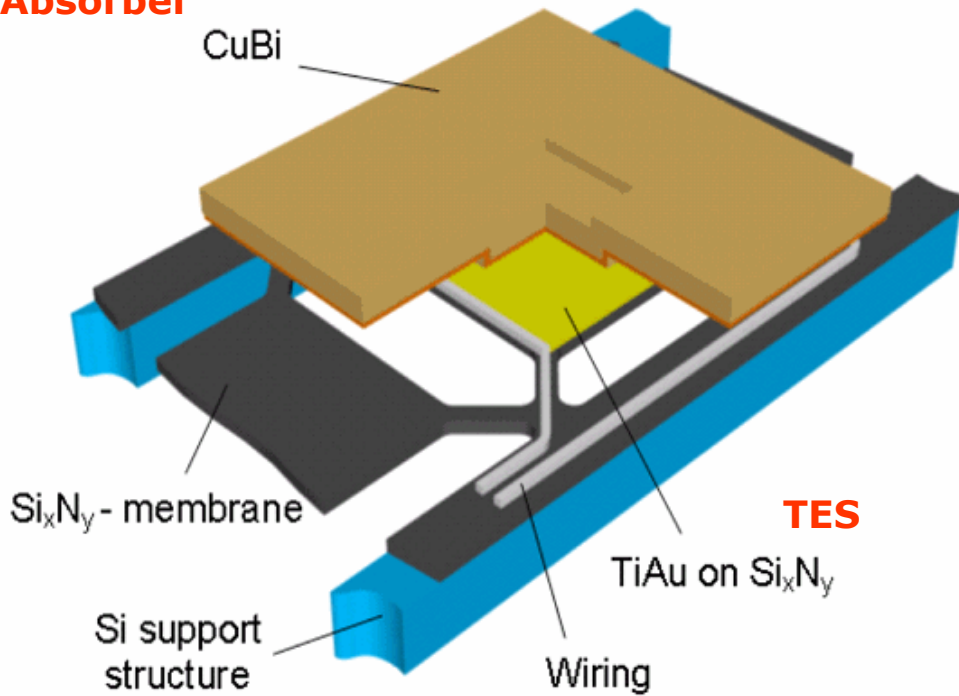


Contents on fabrication

- Pixel components
 - Micro-mechanic support structure
 - TES or Transition Edge Thermometer
 - Absorber
 - Wiring
 - Pixel release
 - Cooling
- Pixel optimization:
 - Trials for steepness/excess noise
 - Avoiding strain concentrations
- Open issues
- Space qualification
- Facilities

Calorimeter pixel components

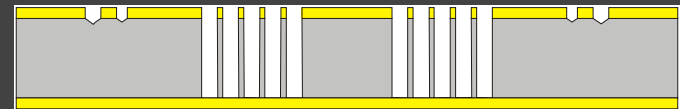
Absorber



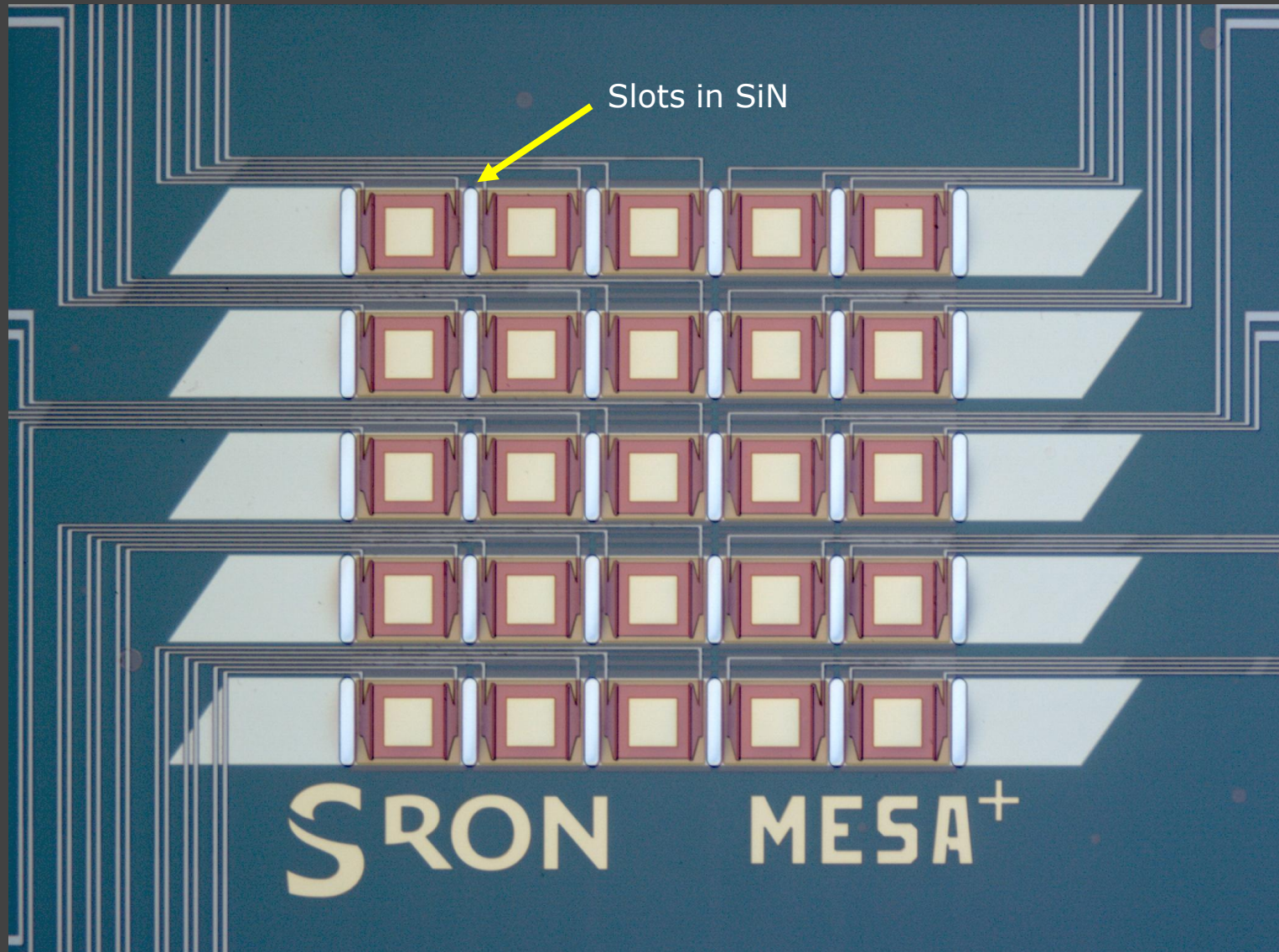
Cooling

Micromechanical support structure

- Fabrication steps:
 - Wafer cleaning Si [110]
 - LPCVD Si₃N₄ coating @ MESA TuE
 - Vangbo alignment pattern (back side)
 - Etching SiN
 - Short KOH etch
 - Slotted pattern (back side)
 - Etching SiN
 - Long KOH etch (full wafer depth)
 - (metal processing)
 - Membrane pattern



5x5 array before absorber and release



TES – Transition Edge Thermometer

Process:

- Sputtercoating of cooling layer (Al) on back side
- Evaporation of Ti/Au/Ti on front side
- Lithography of TES pattern, alignment to back side
- Wet etching
 - Ti: diluted HF
 - Au: I_2/KI , rinse in $Na_2S_2O_3$

Critical issues:

- Wafer handling, protection of backside Al
- Ti/Au deposition (next page)



Ti/Au deposition

- Tc of bi-layer is very sensitive to:
 - Thicknesses
 - Interface condition
 - Purity
 - Temperature $> \sim 100$ C
- **Approach:**
 - Avoid the use of “dirty” materials in the system
 - Clean vacuum
 - Automated deposition sequence with very short delay between Ti and Au (< 2 sec) and reproducible growth rate
 - Cooling of layers on membranes
 - Calibration runs before calorimeter fab.
 - Process accuracy $T_c \pm 15$ mK

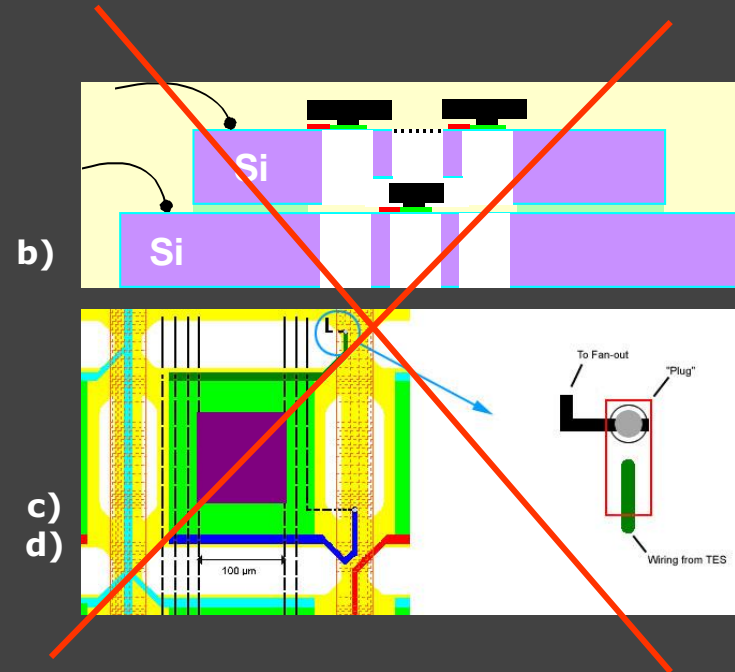


On-chip wiring

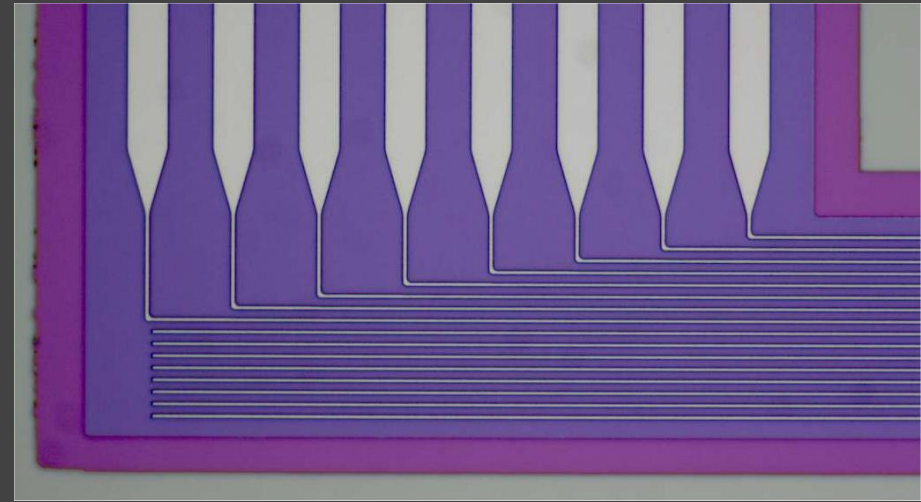
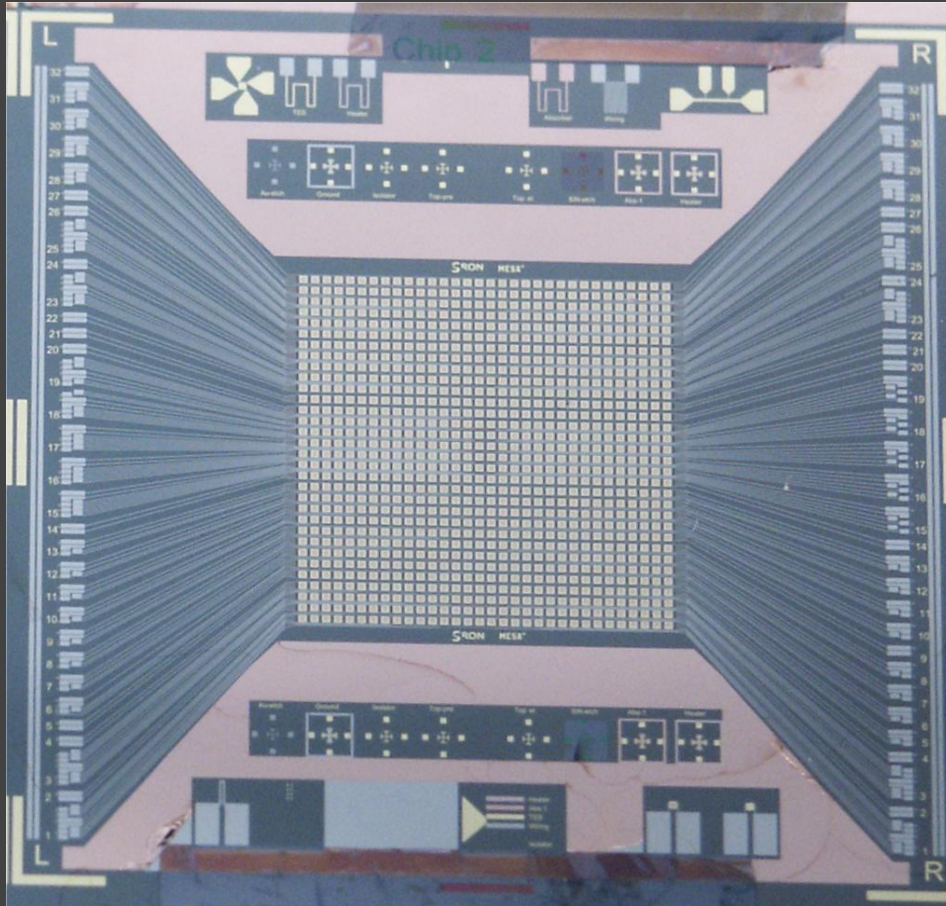
- Wiring issues become especially important for large arrays:
 - Pitch on limited space between pixel rows
 - Yield (shorts & interruptions)
 - Inductance (should be low compared to main FDM inductance)
 - Cross-talk
 - Critical current

- 4 cases were studied:
 - a) (Multi-layer) wiring on the support bars
 - b) Double wafer array
 - c) Wiring under pixel (surface micro-machining)
 - d) Wiring through the wafer

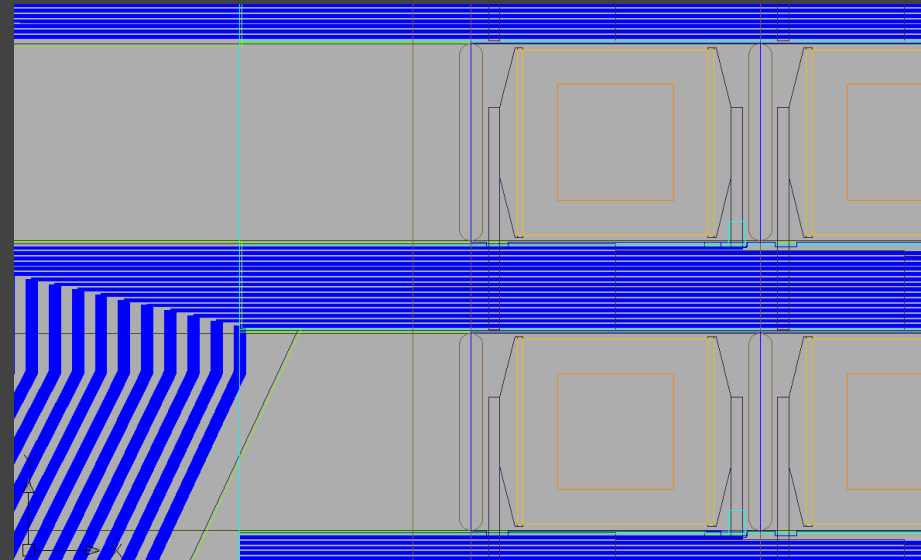
Present choice: case a) seems feasible for 1 kpixel array with $\sim 70 \mu\text{m}$ beams



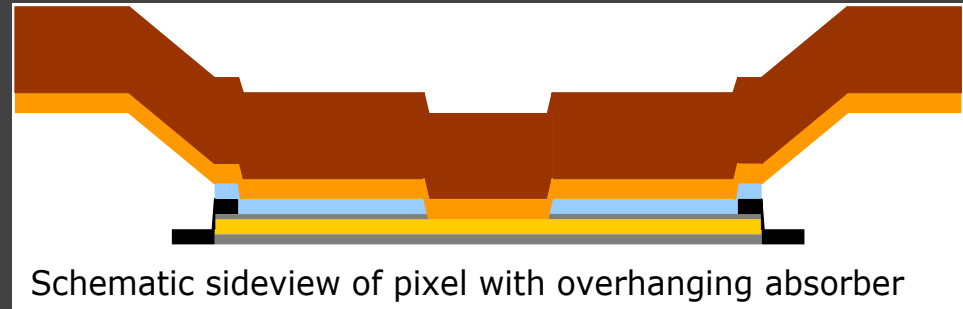
Wiring: Prototype 32 x 32 pixel Array



16 lines on ground plane, pitch 2.8 μm



Absorber fabrication



Formation of photoresist mould



First exposure using an inverted mask, the exposed areas (outside the "hat" pattern) finally remain.



Reversal bake, 2 min on 130 °C cross-links the exposed area while the unexposed area remains photo-active.



Second exposure of the "foot print" in proximity mode to create positive slope. The exposure dose is to generate a high development rate of the exposed (yellow) resist.

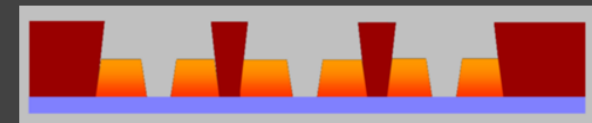


Third exposure is a flood exposure, Exposure dose is low to create selective development rate of the "hat" pattern with respect to the "foot" pattern (yellow).



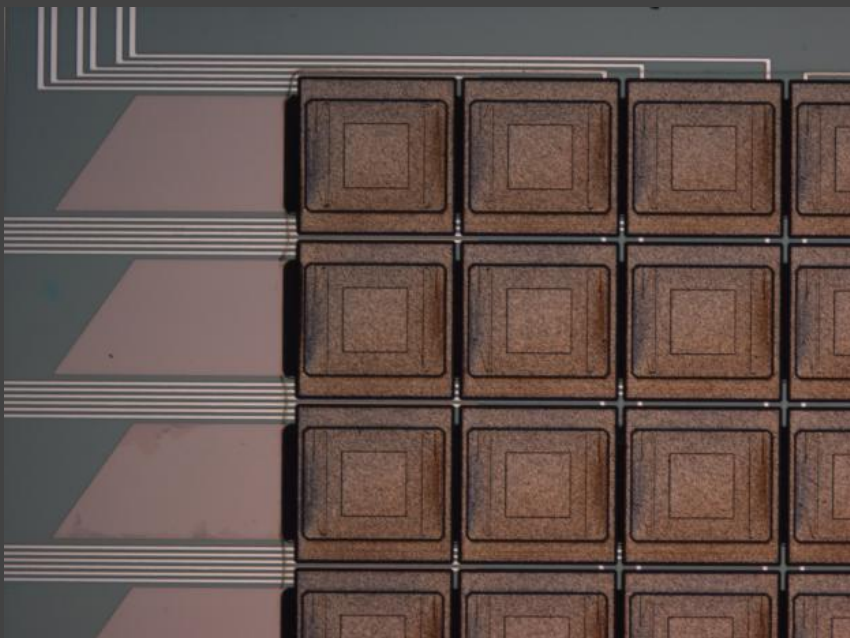
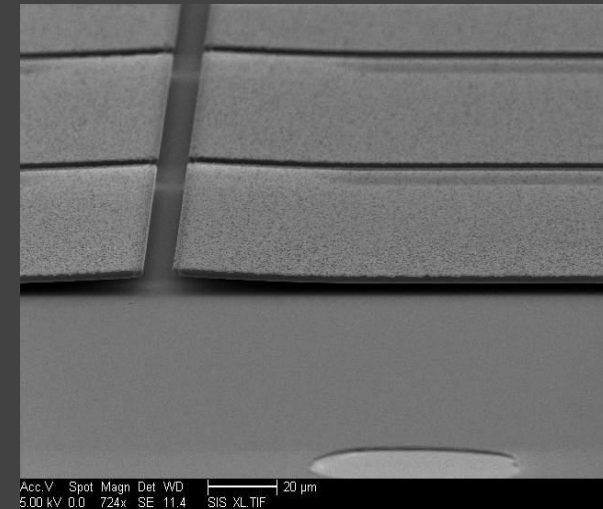
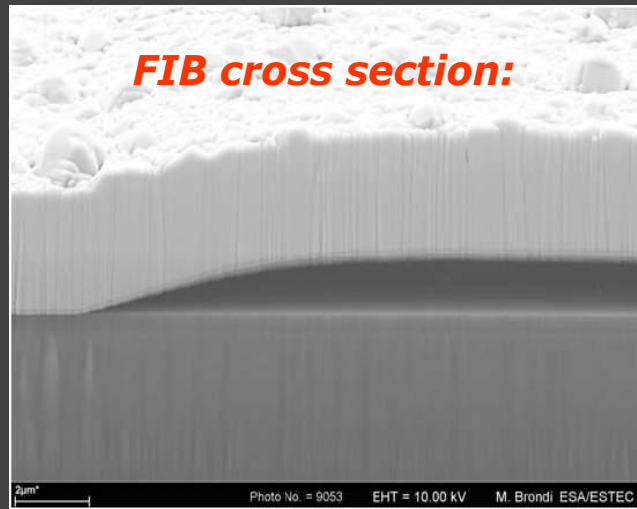
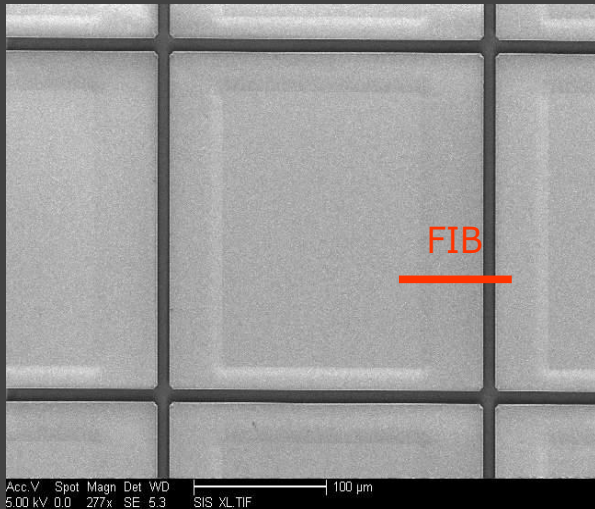
Development of the mushroom shaped mould, the development time is a parameter to adjust the height of the remaining resist which determines the distance between free-hanging absorber hat and the substrate.

Array:



The negative-sloped resist forms the lateral distance between the absorbers hats.

Absorber fabrication



SEM micrographs of mushroom shaped Cu/Bi absorbers.

Upper left: Top view of array on solid Si.

Red line: FIB sectioning.

Upper right: 70° tilted view, showing bending.

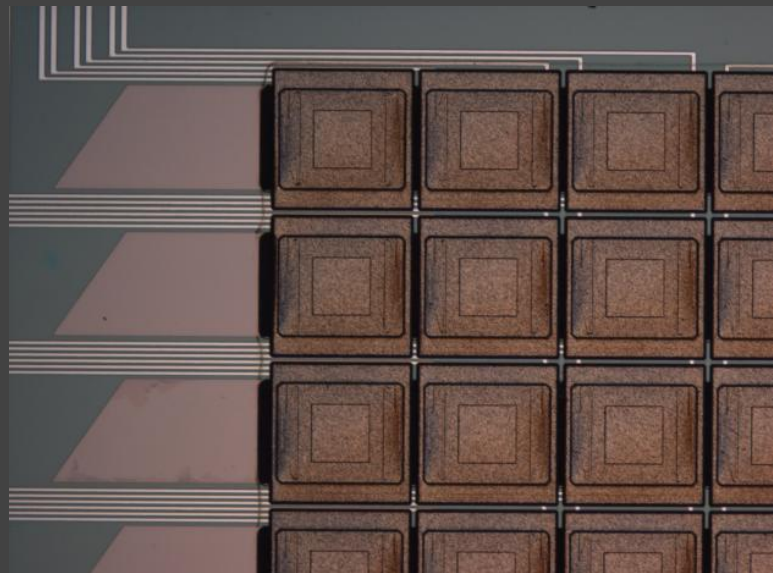
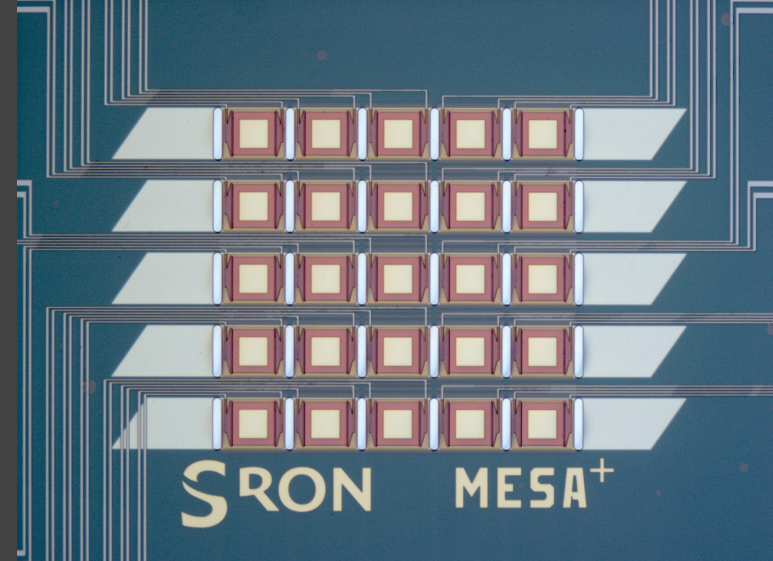
Left: Process on membrane pixels.

Pixel size is 250x250 μm². Filling factor = 93%.

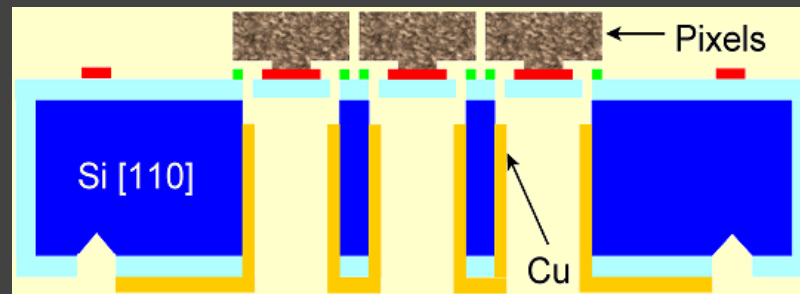
Present Ti/Cu/Bi thickness: 5/150/3000 nm:
Good X-ray performance

Pixel release

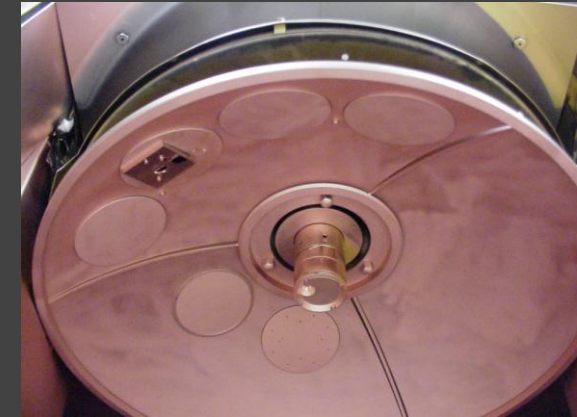
-
 - RIE etching of SiN
 - Resist removal
 - Absorber pattern & deposition
 - Front side resist coating
 - Back side Al etch
 - Lift-off (few hours)
 - Rinsing
 - Drying (face down in oven)
-
- ❖ Tricky handling
 - ❖ Avoid loss of Cu below Bi
 - ❖ Avoid sticking of absorber to substrate



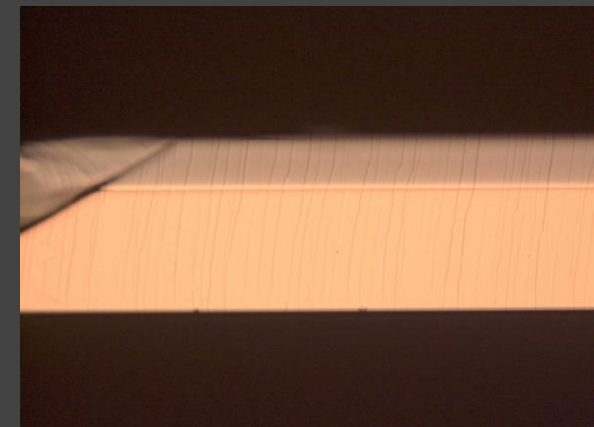
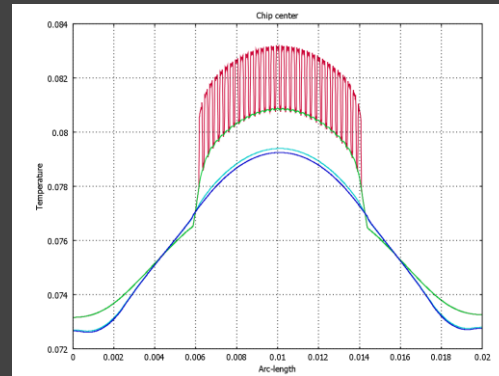
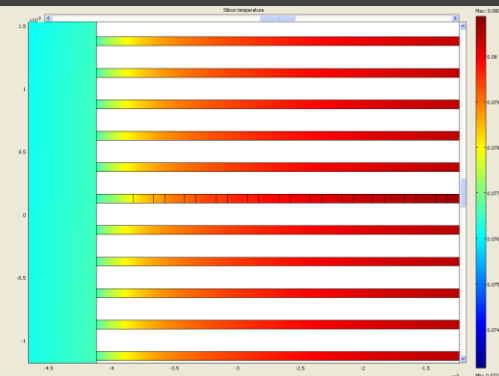
Cooling



- Heat conduction of Si beams insufficient for bias power removal
- Cu is shadow evaporated onto sides of the beams and back side of chip
- Simulations and experiments confirm vastly improved conduction
- Thermal cross talk is reduced



Adjustable angle in evaporator



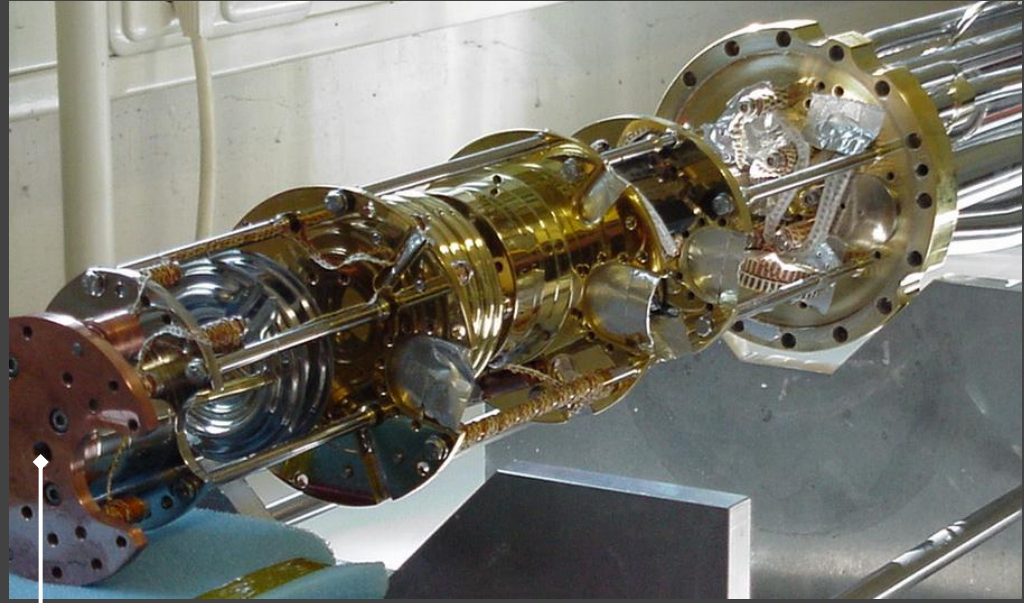
Side view on (broken) beam

Setup's for single pixel characterization

Kelvinox dilution fridge



the insert



mounting position for bracket with samples

For the moment FDM takes only place in ADR



EMC/GROUNDING/HARNESS/FILTERING

Esperiment set-up

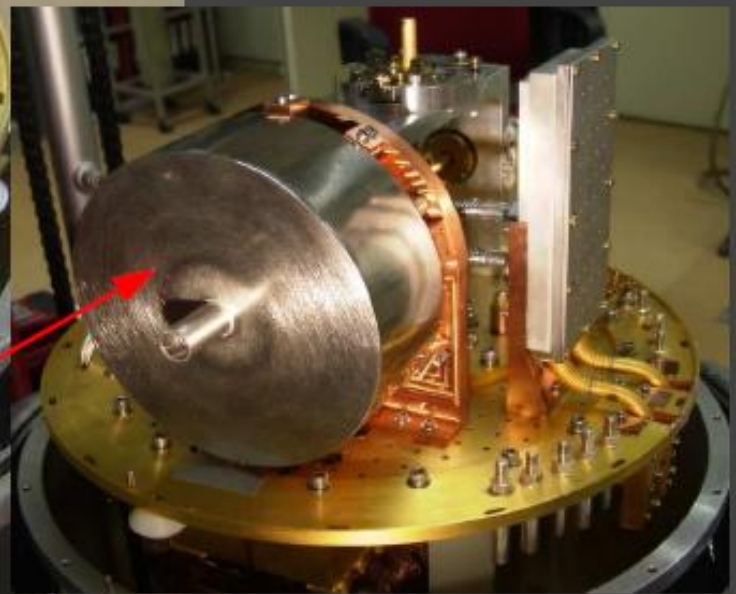
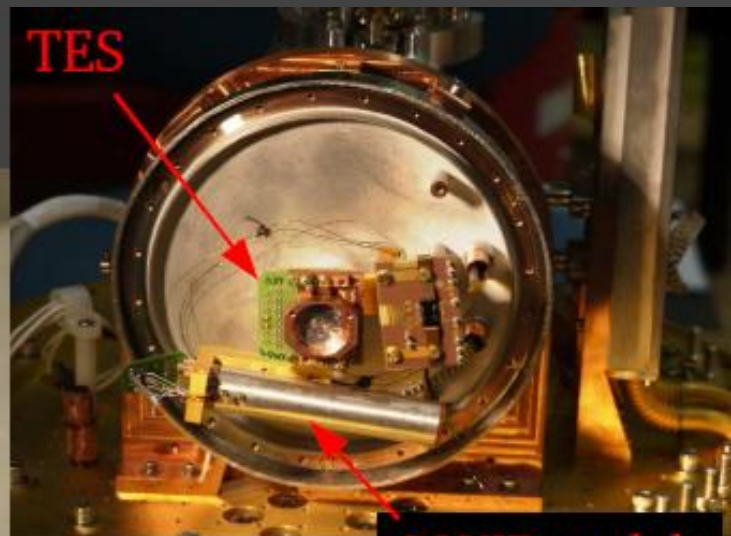
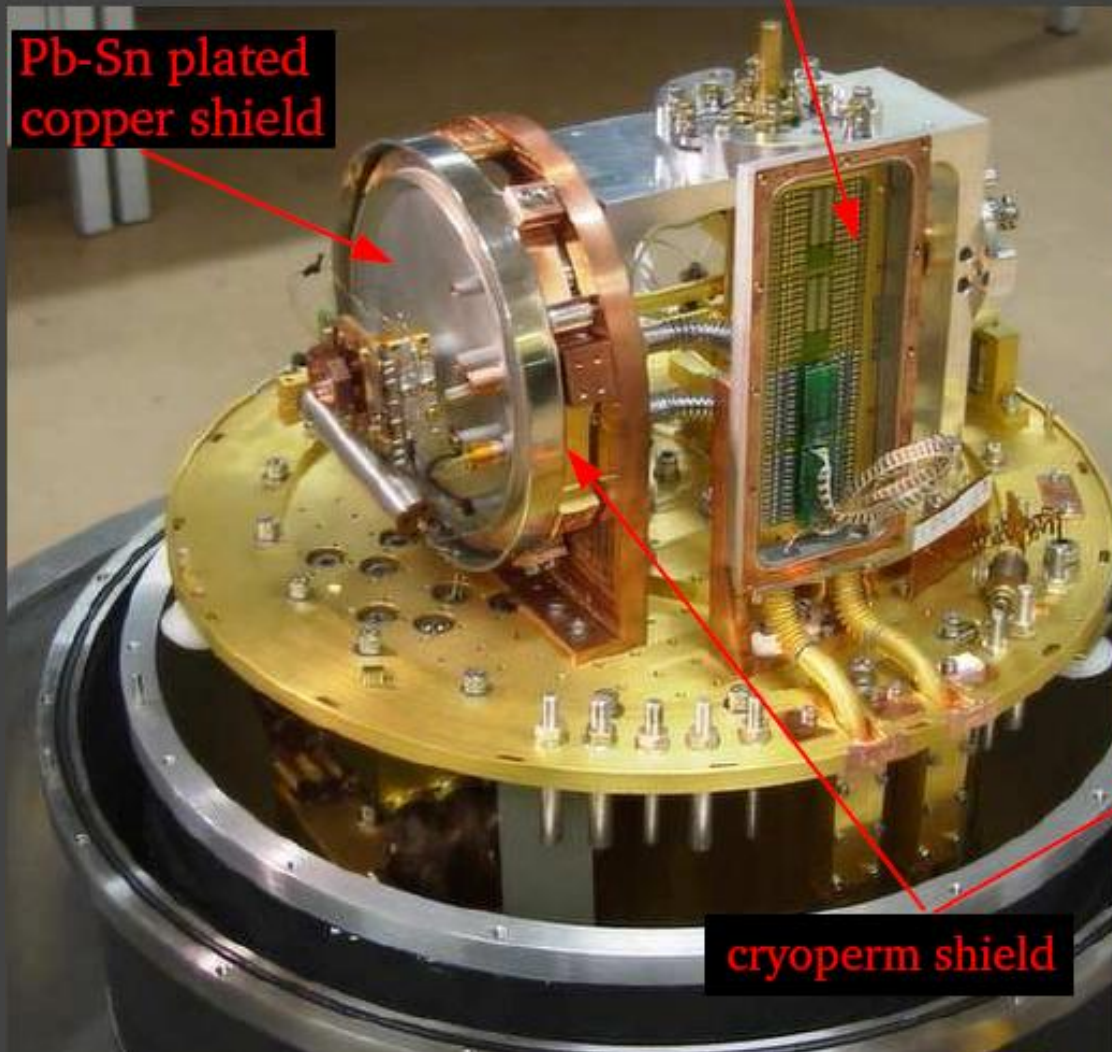
4K filter board

TES

Pb-Sn plated copper shield

SQUID module

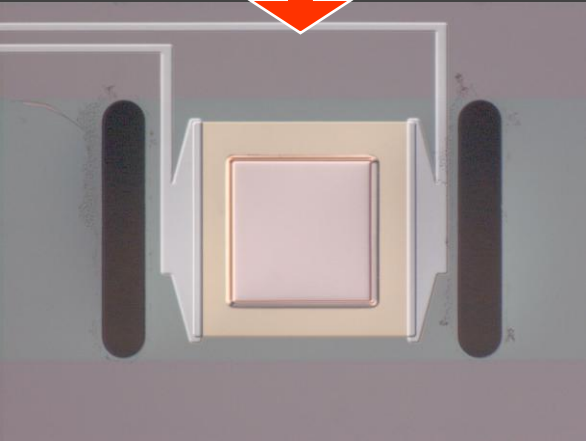
cryoperm shield



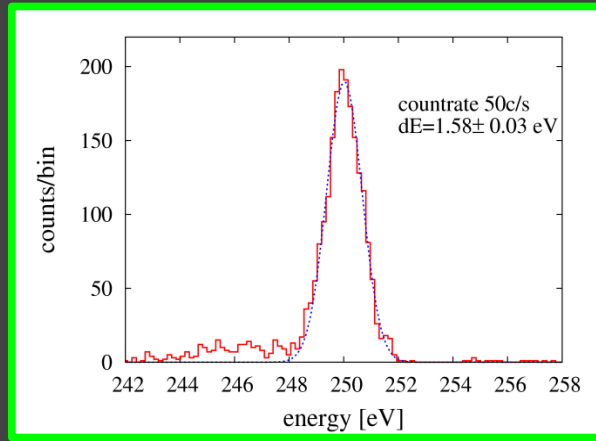
Narrow Field Imager - TES-based Micro-Calorimeter

PERFORMANCE for PIXELS from 5 x 5 arrays

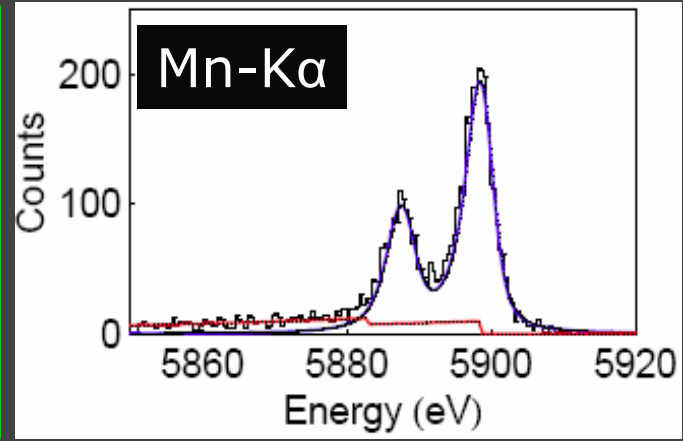
$\Delta E_{TDL} \approx 3.1$ eV



Cu-absorber



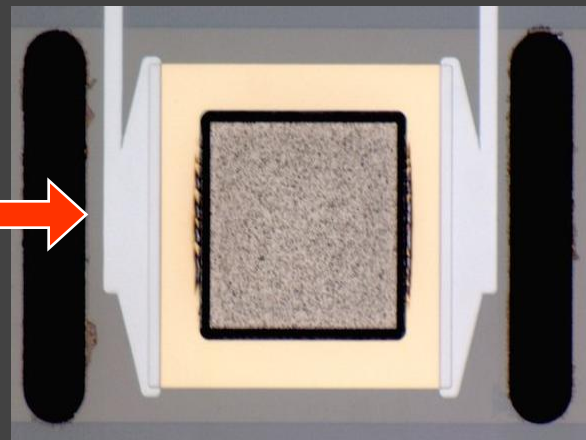
$\Delta E = 1.6$ eV @ 250eV



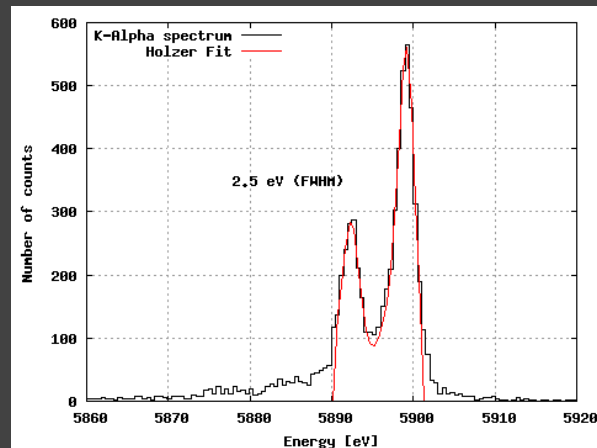
$\Delta E = 2.9$ eV at 5.9 keV

100 μ s fall time

$\Delta E_{TDL} \approx 3.8$ eV



Cu/Bi-absorber



$\Delta E = 2.5$ eV @ 5.9 keV

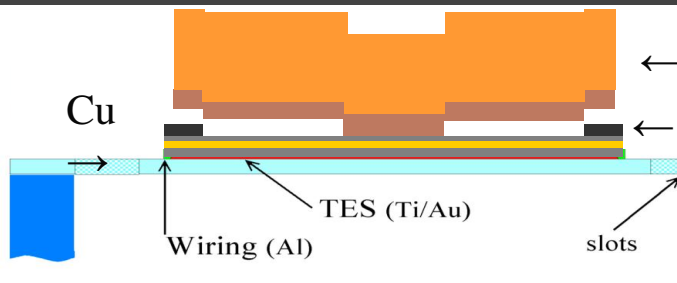
$$\Delta E_{TDL} = 2.35 \sqrt{k_B T^2 C}$$

Narrow Field Imager - TES-based Micro-Calorimeter

PERFORMANCE for PIXELS from 5 x 5 arrays

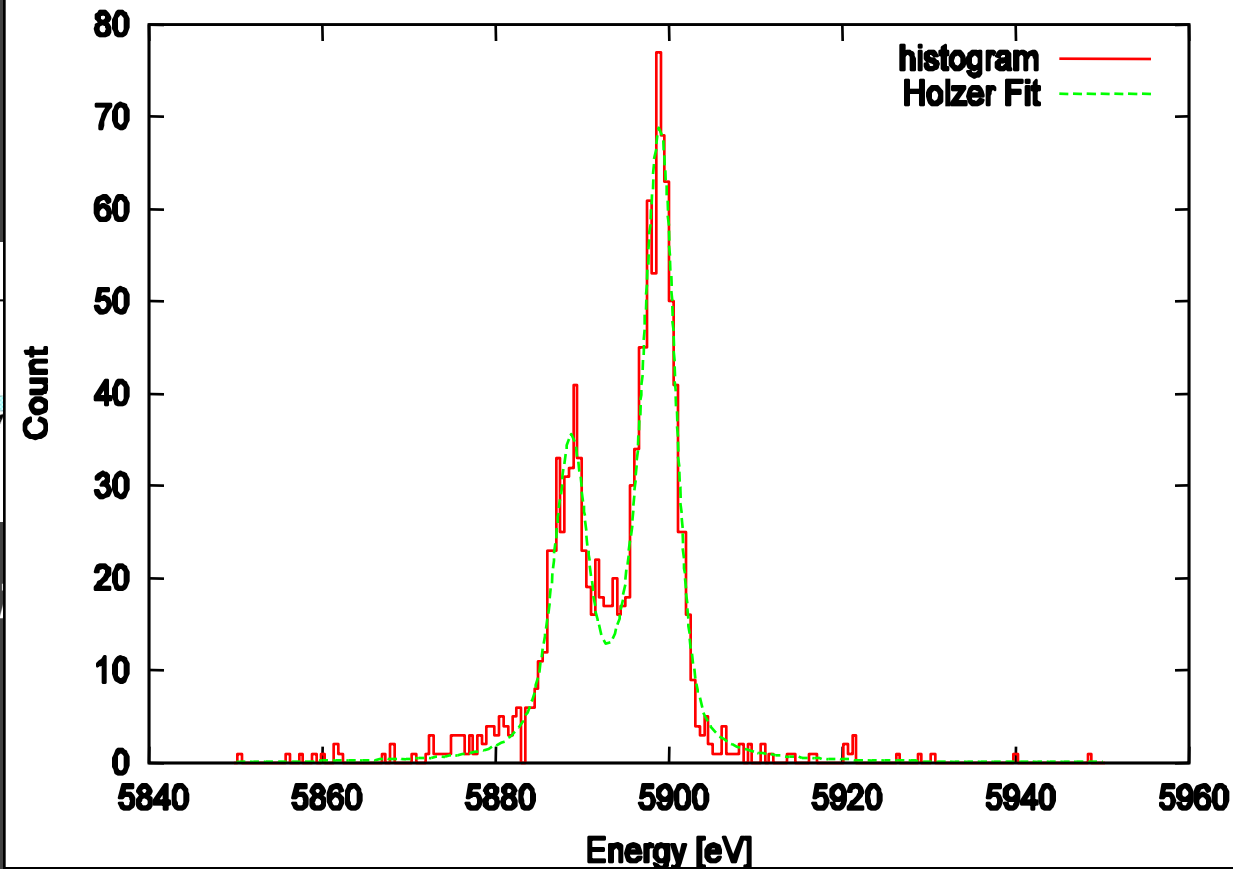
$$\Delta E_{TDL} = 2.35 \sqrt{k_B T^2 C}$$

$$\Delta E_{TDL} \approx 4.4 \text{ eV}$$



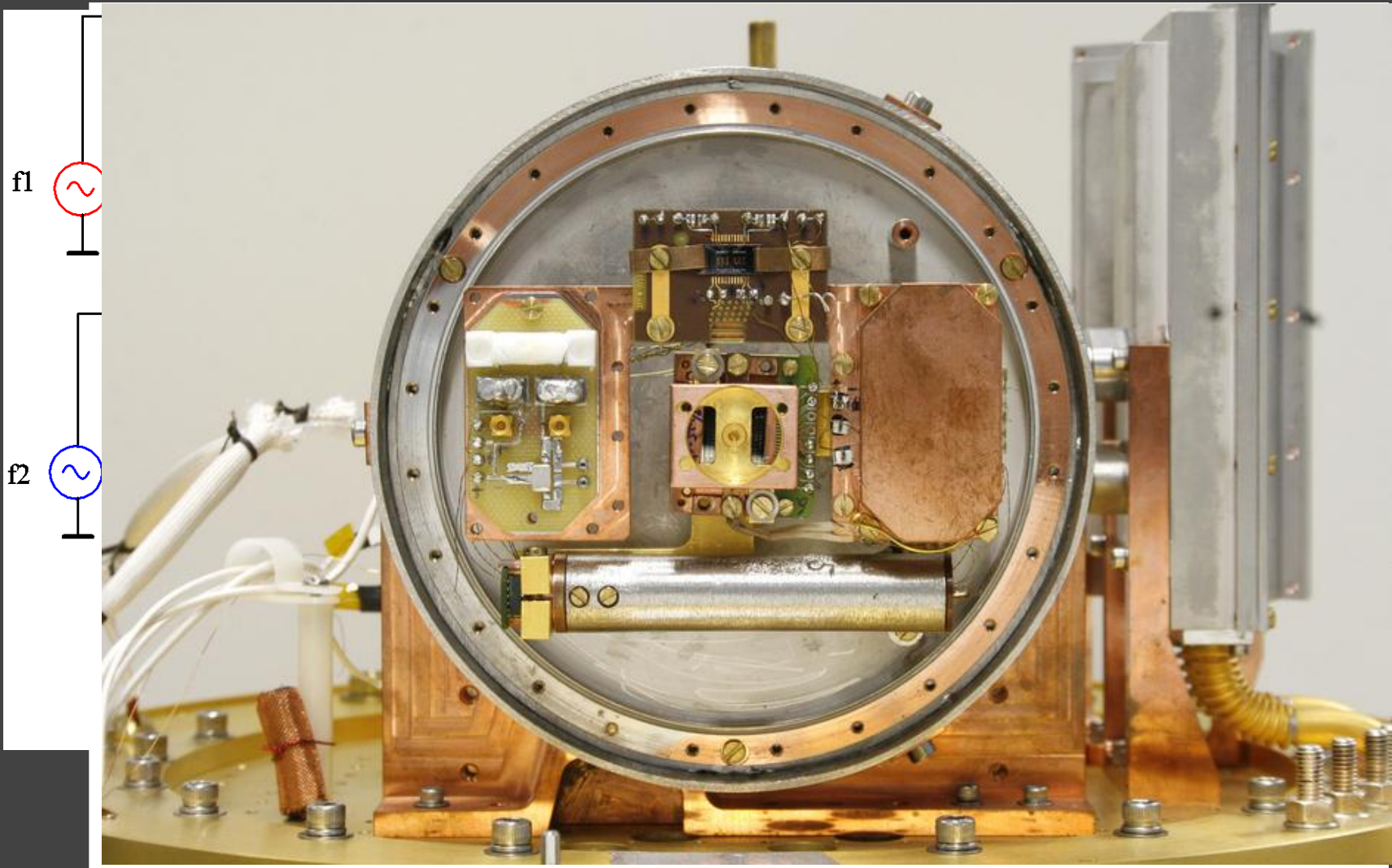
Cu/Bi-absorber (0.3/3 μm)
 $T_C = 116 \text{ mK}$

K-Alpha Spectrum of TT086-25-kw2-chip4-pix6 (2000 pulses, 3.10823 eV)



$\Delta E = 3.1 \text{ eV @ } 5.9 \text{ keV}$
200 μs fall time

FREQUENCY DOMAIN MULTIPLEXING CURRENT SUMMING TOPOLOGY



ts



20

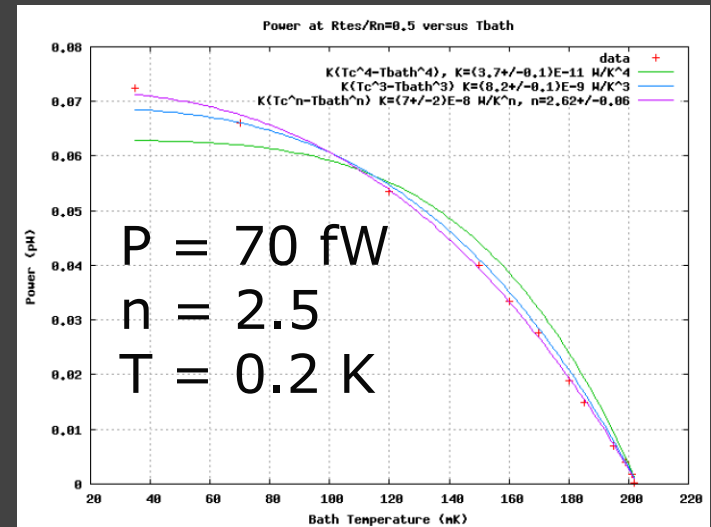
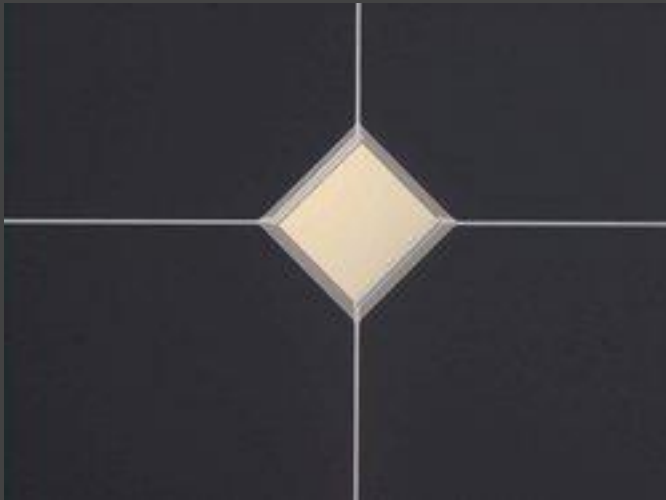
TES

rease
rize
ease

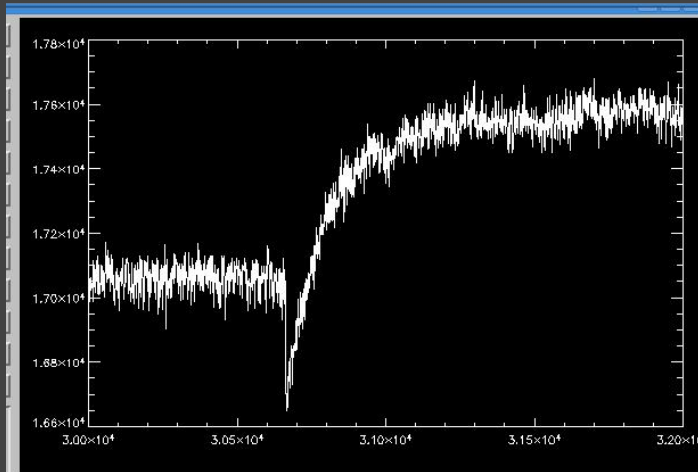
e
will
45

enable multiplexing of 25
pixels/channel

Low NEP TES for SAFARI/SPICA



$$NEP = \sqrt{4kT^2 P} \approx \sqrt{4kTP}$$



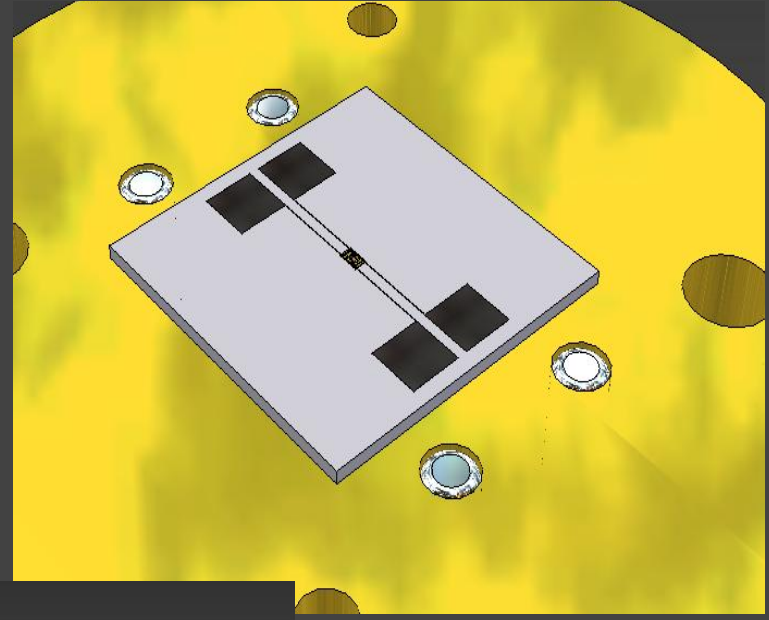
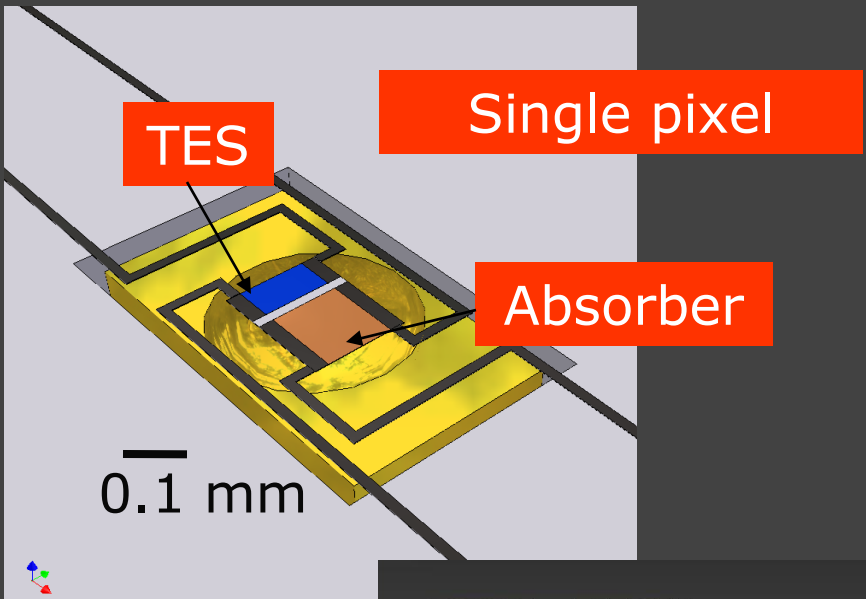
$T_c = 200$ mK
 100×100 μ m TES
 4 legs of 5 μ m and
 1.8 mm

Measured
 $P = 70$ fW
 $NEP = 10^{-18}$ W/ \sqrt Hz
 $\tau_{eff} = 0.2$ ms

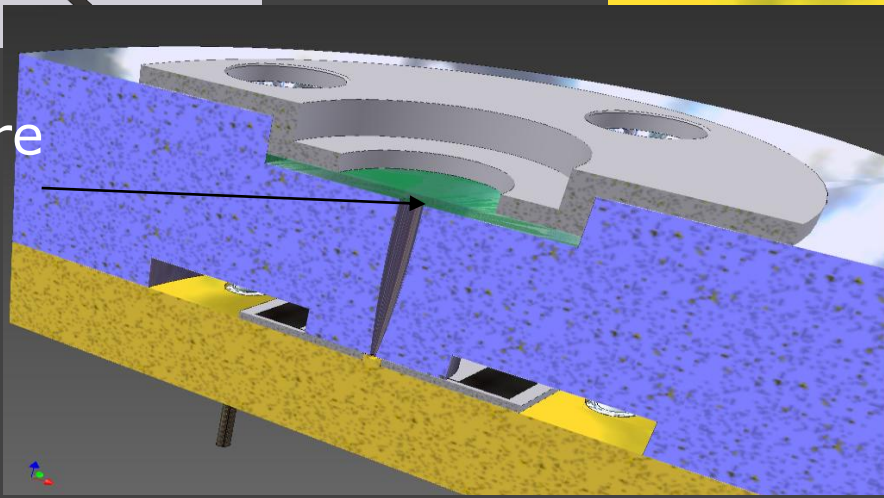
Next steps:

$T \rightarrow 100$ mK
 Leg width $\rightarrow 2$ μ m

Single optical pixel design (short wavelength channel is most difficult)

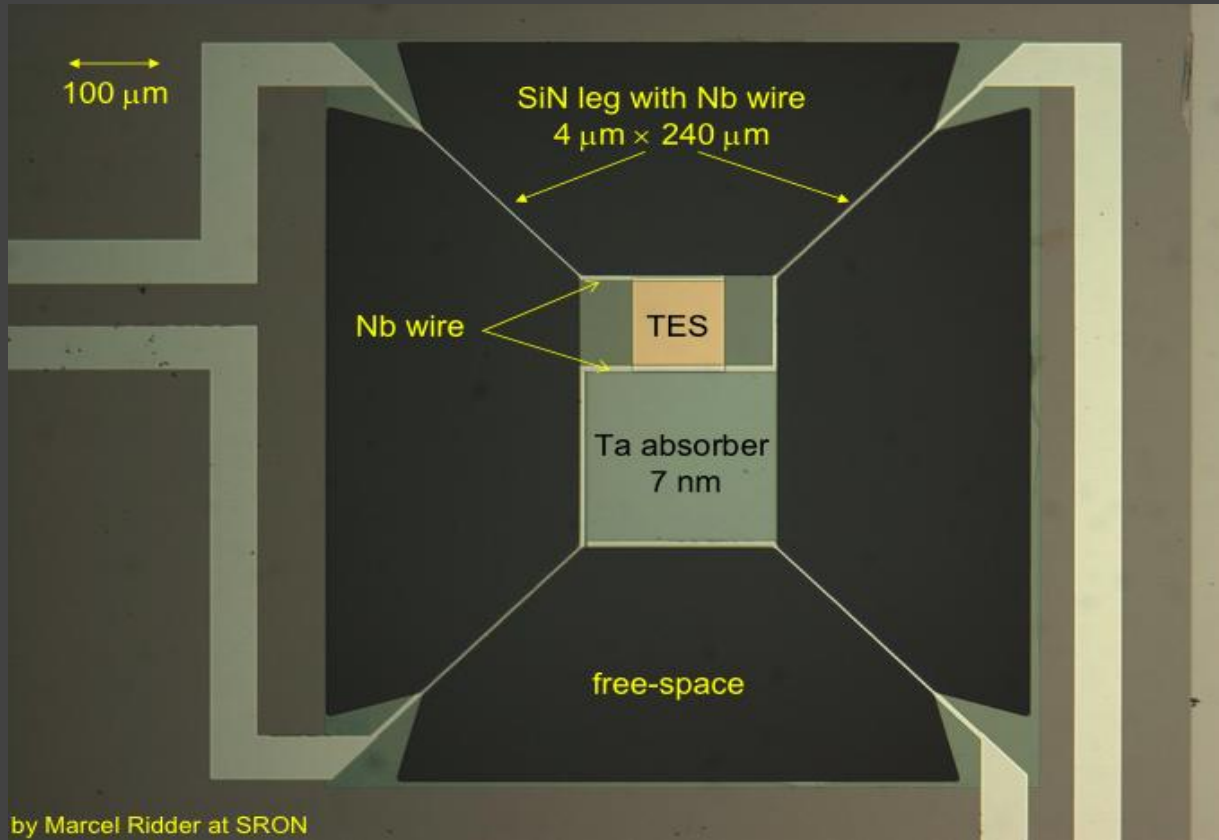


Horn aperture is 450 μm



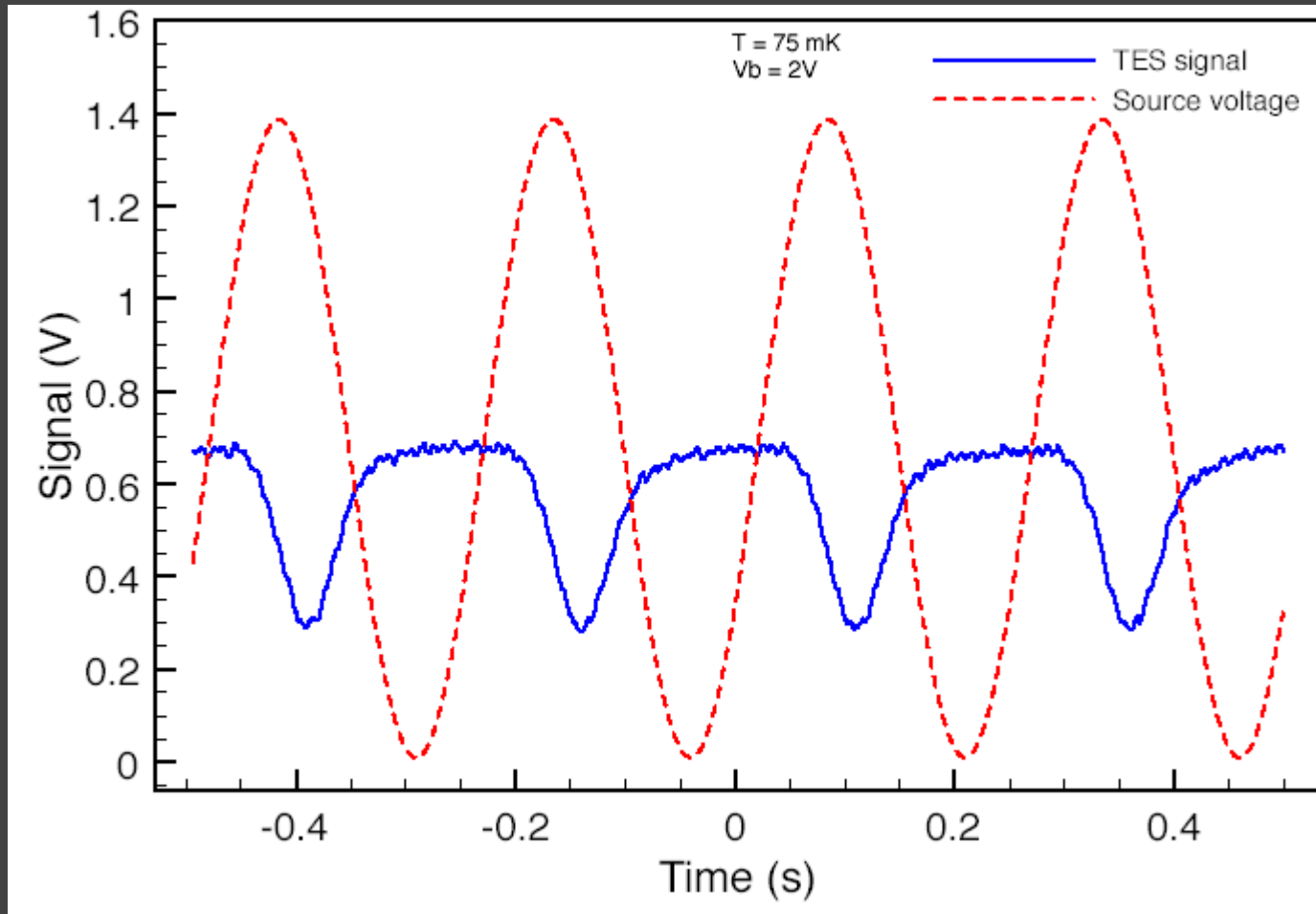
Example: 11 mm test chip size

Single pixel with optical absorber (a real picture)



Free space 400 Ohms per square absorber coupled to TES
First devices fabricated and undergoing dark testing
Optical testing ready to begin

It works!!!



Absorbers fed by circular horn antennas
Integrating metal backshort